

# Analytical Calculation of Four-Point Correlations for a Simple Model of Cages Involving Numerous Particles

Ooshida Takeshi\*

*Department of Mechanical and Aerospace Engineering, Tottori University, Tottori 680-8552, Japan*

Susumu Goto

*Graduate School of Engineering Science, Osaka University, Toyonaka, Osaka 560-8531, Japan*

Takeshi Matsumoto

*Division of Physics and Astronomy, Graduate School of Science, Kyoto University, Kyoto 606-8502, Japan*

Akio Nakahara

*Laboratory of Physics, College of Science and Technology,  
Nihon University, Funabashi, Chiba 274-8501, Japan*

Michio Otsuki

*Department of Physics and Mathematics, Aoyama Gakuin University, Sagami-hara, Kanagawa 229-8558, Japan*

(Dated: January 23, 2013)

Dynamics of one-dimensional systems of Brownian particles with short-range repulsive interaction (diameter  $\sigma$ ) is studied with a liquid-theoretical approach. The mean square displacement, the two-particle displacement correlation, and the overlap-density-based generalized susceptibility are calculated analytically by way of the Lagrangian correlation of the interparticulate space, instead of the Eulerian correlation of density that is commonly used in standard mode-coupling theory. In regard to the mean square displacement, the linear analysis reproduces the established result on the asymptotic subdiffusive behavior of the system. A finite-time correction is given by a Lagrangian version of mode-coupling theory. The notorious difficulty in derivation of mode-coupling theory concerning violation of the fluctuation-dissipation theorem is found to disappear by virtue of the Lagrangian description. The Lagrangian description also facilitates analytical calculation of four-point correlations in the space-time, such as the two-particle displacement correlation. The two-particle displacement correlation, which is asymptotically self-similar in the space-time, illustrates how the cage effect confines each particle within a short radius on one hand and creates collective motion of numerous particles on the other hand. As the time elapses, the correlation length grows unlimitedly, and the generalized susceptibility based on the overlap density converges to a finite value which is an increasing function of the density. The distribution function behind these dynamical four-point correlations and its extension to three-dimensional cases, respecting the tensorial character of the two-particle displacement correlation, are also discussed.

## I. INTRODUCTION

In spite of the ever more active studies on glassy systems in the last few decades [1, 2], and even after the discovery of dynamical heterogeneity [3, 4], theoretical understanding of jamming, plasticity, and glass transition remains a challenging problem in statistical physics. The dynamical heterogeneity in glassy systems refers to the presence of non-trivial collective motion of numerous particles with some correlation length and lifetime; the growth of this *dynamical* correlation length, as opposed to the static correlation which has been sought fruitlessly, is now considered to account for the slowdown of the dynamics near the glass transition. However, kinetic-theoretical treatment of this collective motion is formidably difficult, as its correct description requires a

four-point correlation function, whose analytical calculation has been infeasible except for some special cases such as kinetically constrained models on a lattice [5]. Indeed, a growing dynamical length in supercooled liquids was recently calculated [6] by extending a prevalent theoretical scheme known as the mode-coupling theory (MCT) [7], but MCT suffers from its own difficulties [8, 9]. Besides, it is not clear how the cage effect, which confines each liquid particle within a short radius, is related to the long-ranged dynamical correlation.

In such a state of affairs, what Hilbert said in his well-known speech [10] is thought-provoking. Emphasizing the vital role of good problems that serve to temper the sword of mathematical methodology, he pointed out the importance of proper specialization: in order to overcome mathematical difficulty, we should study “problems simpler and easier than the presented one” in depth. In solving the specialized, “simpler and easier” problems, one has a chance of developing an innovative method with generalizable concepts, which eventually makes it

---

\*E-mail: ooshida@damp.tottori-u.ac.jp

possible to overcome the original difficulties.

In our case, the “presented problem” is to elucidate the nature of the slow dynamics characterizing glassy systems, by extracting an effective theory for it from their particle-scale models. To be specific, let us consider dense colloid suspensions, modeled as a three-dimensional system of interacting Brownian particles:

$$m\ddot{\mathbf{r}}_i = -\mu\dot{\mathbf{r}}_i - \frac{\partial}{\partial \mathbf{r}_i} \sum_{j < k} V(r_{jk}) + \mu \mathbf{f}_i(t), \quad (1.1)$$

$$\langle \mathbf{f}_i(t) \otimes \mathbf{f}_j(t') \rangle = \frac{2k_B T}{\mu} \delta_{ij} \delta(t - t') \mathbb{1}. \quad (1.2)$$

Without the interaction ( $V = 0$ ), the statistically averaged or coarse-grained density field would be governed by the simple diffusion equation, with the diffusion constant  $D = k_B T / \mu$ . Contrastively, for repulsive short-range interaction potentials with excluded volume effect that determines the particle diameter  $\sigma$  (and with some contrivance to avoid crystallization), the Monte Carlo and molecular-dynamical equivalents of Eq. (1.1) show glassy behavior [11, 12]. As the density increases, the cages have stronger effect, which results in the extremely slow relaxation of the intermediate scattering function  $F(\mathbf{q}, t) \propto \langle \hat{\rho}(\mathbf{q}, t) \hat{\rho}(-\mathbf{q}, 0) \rangle$ , with  $\hat{\rho}$  denoting the Fourier component of the density, such that

$$\rho(\mathbf{r}, t) = \sum_j \delta(\mathbf{r} - \mathbf{r}_j(t)) = \rho_0 + \sum_{\mathbf{q}} \hat{\rho}(\mathbf{q}, t) e^{-i\mathbf{q} \cdot \mathbf{r}}. \quad (1.3)$$

The slowdown of the dynamics suggests the presence of some spatial structure with growing scale, but this is not detectable via the static structure factor,  $S(\mathbf{q}) = F(\mathbf{q}, 0)$ . Instead, a cooperative motion with growing correlation length is evidenced by four-point dynamical correlations [13, 14], such as

$$\chi_4(t) \propto \iint \left[ \langle \rho(\mathbf{r}_1, t) \rho(\mathbf{r}_1, 0) \rho(\mathbf{r}_2, t) \rho(\mathbf{r}_2, 0) \rangle - \langle \rho(\mathbf{r}_1, t) \rho(\mathbf{r}_1, 0) \rangle \langle \rho(\mathbf{r}_2, t) \rho(\mathbf{r}_2, 0) \rangle \right] d^3 \mathbf{r}_1 d^3 \mathbf{r}_2.$$

In particle-based computations, it is evaluated typically via the overlap density

$$\mathcal{Q}(t) = \sum_i \sum_j \bar{\delta}_a(\mathbf{r}_i(0) - \mathbf{r}_j(t))$$

as

$$\chi_4(t) \propto \langle \mathcal{Q}(t)^2 \rangle - \langle \mathcal{Q}(t) \rangle^2, \quad (1.4)$$

with  $\bar{\delta}_a$  denoting the overlapping function, which has a finite value around  $r = 0$  and vanishes for  $r \gg a$ . The spatiotemporal structure, characterized by four-point space-time correlations, is referred to as dynamical heterogeneity and now studied intensively [4], in the hope of finding the secret of the glassy dynamics in it. Nevertheless, calculation of dynamical four-point correlations for

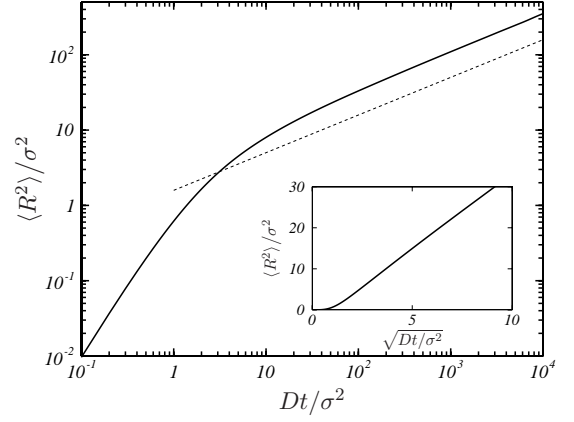


FIG. 1: The mean square displacement  $\langle R^2 \rangle$  in SFD, plotted as a function of  $t$ . The dotted line indicates the slope for  $t^{1/2}$ . The system size is specified as  $N = 2^{15} = 32768$  and  $\rho_0 = N/L = 0.25 \sigma^{-1}$ . In the inset, the same  $\langle R^2 \rangle$  is plotted against  $\sqrt{t}$  for  $0 < \sqrt{Dt} < 10 \sigma$ .

Eq. (1.1) is so difficult that, to our knowledge, no one has managed to calculate them analytically. The theoretical calculation of  $\chi_4$  by Donati *et al.* [15] concerns the static case. The most remarkable success was made by Toninelli *et al.* [5], who calculated  $\chi_4$  analytically for elastic solids and kinetically constrained lattice models. These are cases in which permanent “bonds” are present: the situation is different in the colloidal system governed by Eq. (1.1), which lacks such “bonds” connecting the particles (at least explicitly). Besides, it should be emphasized that MCT [7, 8] targets on the dynamical structure factor  $F(\mathbf{q}, t)$  and not on four-point correlations. As long as the standard variables such as  $\hat{\rho}(\mathbf{q}, t)$  in Eq. (1.3) are used, a *four-point* correlation function implies a *four-body* correlation. Since MCT is a closure theory in which quadruple (four-body) correlations are approximated by products of  $F$ , it is unlikely to describe four-point correlations accurately, for example, with the accuracy needed for treatment of entanglement effects in melts of rod polymers [16]. Although a calculation of three-point correlation within the MCT approximation was recently reported [6], still  $\chi_4$  remains insurmountable.

With this situation in mind, according to Hilbert’s advice, let us look for “simpler and easier” problems that may give insight into real glassy systems. Instead of Eq. (1.1), here we study its one-dimensional version:

$$m\ddot{X}_i = -\mu\dot{X}_i - \frac{\partial}{\partial X_i} \sum_{j < k} V(X_k - X_j) + \mu f_i(t) \quad (1.5)$$

whose behavior is known by the name of *single-file diffusion* (SFD) [17–25]. For  $V$  we adopt a *short-ranged* repulsive potential, such as Eq. (A1) in Appendix A, so that the system exhibits a liquid-like structure factor [26, 27]. Despite this retainment of the original feature of Eq. (1.1), since the one-dimensional system does not

exhibit glass transition, Eq. (1.5) may seem less than a toy model for studies of glassy dynamics. This is a superficial view, however, if we note that SFD throws one of the difficulties of MCT into relief—the difficulty met by Miyazaki and Yethiraj [16] in their study of rod polymers, for which they needed to go beyond the standard MCT by directly calculating the four-point correlation, as will be explained later.

It is also a kind of four-point correlation function that we treat here to account for the slow diffusion subject to Eq. (1.5). By “slow” we mean that SFD is subdiffusive [19, 20]: by observing longtime behavior of the mean square displacement (MSD), denoted by  $\langle R_j^2 \rangle$  with

$$R_j = R_j(t) = X_j(t) - X_j(0), \quad (1.6)$$

it is found that  $\langle R_j^2 \rangle$  for SFD behaves like  $\sqrt{t}$  [see Eq. (1.7) shown later], which is slower than  $\langle R_j^2 \rangle \propto t$  expected for the normal diffusion. The subscript in  $\langle R_j^2 \rangle$  can be omitted as we assume that the system is statistically uniform. The subdiffusive law,  $\langle R^2 \rangle \propto \sqrt{t}$ , is readily confirmed by simulation of a system with  $N$  particles in a periodic box of the size  $L$ . In the calculations shown in Fig. 1, the mean density,  $\rho_0 = N/L$ , equals  $0.25 \sigma^{-1}$ , and the system is statistically steady. For computational details, see Appendix A. The finite size effect is eliminated by taking sufficiently large  $L$  and interpreting the word “longtime” as  $\rho_0^{-2} \ll Dt \ll L^2 \rightarrow \infty$ . For the longtime regime in this sense, Kollmann showed [20]

$$\langle R^2 \rangle = \frac{2S}{\rho_0} \sqrt{\frac{D_c t}{\pi}} \propto t^{1/2}, \quad (1.7)$$

where  $S = S(0)$  denotes the long wave limiting value of the static structure factor  $S(k)$ , and  $D_c$  is the collective diffusion constant. We note that Kollmann also needed to calculate a kind of four-point correlation ( $\kappa^{(2)}$  in his notation) in derivation of Eq. (1.7).

The slowness of SFD is ultimately due to the presence of the repulsive potential term in Eq. (1.5). The structure of Eq. (1.5) is basically the same as that of the three-dimensional equation (1.1), except for the geometrical difference that makes the cages temporary in the three-dimensional systems while the one-dimensional cages are eternal. Then there is a question: Does a straightforward application of MCT to Eq. (1.5) reproduce the subdiffusive law (1.7)? Unfortunately, the answer is negative according to Miyazaki [9, 28], who demonstrated that MCT predicts normal diffusion,  $\langle R^2 \rangle \propto t$ , instead of  $t^{1/2}$ . His results imply that the dynamical constraint by the long-lived cages is not described accurately enough by the standard MCT. Essentially the same difficulty occurs in MCT for rod polymers [16], as it predicts that the self-diffusion coefficient becomes isotropic for large aspect ratio and therefore fails to describe the entanglement effects.

Motivated by Miyazaki’s study on SFD [9, 28] and also inspired by the notion of Lagrangian correlation in clo-

sure theories of fluid turbulence [29–32], the present authors reformulated the continuum theory of SFD with the *label variable* [24]. This is essentially an application of the Lagrangian description [33, 34], as opposed to the Eulerian, to the Langevin equation for the density field. The label variable method made it possible to reproduce the subdiffusive law (1.7), with the correct power and correct coefficient.

In the present paper, we demonstrate that the label variable method allows us to calculate four-point correlations explicitly. It is demonstrated by generalizing the calculation of MSD [24] to the *two-particle displacement correlation* (2pDC),

$$\langle R_i R_j \rangle = \langle [X_i(t) - X_i(0)] [X_j(t) - X_j(0)] \rangle. \quad (1.8)$$

Quantities analogous to 2pDC have been studied by a number of researchers [12, 35–37] with numerical data from molecular dynamics, and it is also the main ingredient of the theory of  $\chi_4$  for elastic waves by Toninelli *et al.* [5]. Nevertheless, analytical calculations of 2pDC for “bondless” particle systems have never been reported. Here we calculate 2pDC *analytically* in terms of generalizable and liquid-oriented concepts, so that the theory could be extended to truly bondless systems in the near future. At first, we calculate 2pDC as a function of the elapsed time  $t$  and some properly defined label distance which coincides with  $|i - j|$  in the one-dimensional cases; and subsequently, we show it to be re-expressible as a function of  $t$  and the initial distance  $\tilde{d} = X_j(0) - X_i(0)$ , which we denote with  $X_R(\tilde{d}, t)$ . For  $i = j$ , Eq. (1.8) reduces to MSD. The two-particle correlation,  $\langle R_i R_j \rangle$  with  $i \neq j$ , provides an intuitive form of four-point correlation in comparison to  $\chi_4$ ; the 2pDC with  $i \neq j$  vanishes for free Brownian particles and, for SFD, evidences the cluster size that behaves like  $\rho_0 \sqrt{D_c t}$ , accounting for the slow diffusion. In addition, from the knowledge of  $\langle R_i R_j \rangle$ , we can perform a fully analytical calculation for the self part of  $\chi_4$ , defined as

$$\chi_4^S(t) \propto \langle Q_S^2 \rangle - \langle Q_S \rangle^2,$$

where  $Q_S = \sum_i \delta_a(R_i(t))$  [see Eq. (5.9) in Sec. V for details]. Reflecting the eternity of the one-dimensional cages, the longtime limiting value,  $\chi_4^S(+\infty)$ , is finite, as will be shown in Eq. (5.17).

Furthermore, we demonstrate that an MCT-like nonlinear theory for the fluctuation of  $1/\rho$  can be developed in a field-theoretical style, without violating the fluctuation-dissipation theorem (FDT). This is possible because the problem of the multiplicative noise is naturally resolved by virtue of the label variable. The contribution of the memory term gives a finite-time correction to Kollmann’s asymptotic result (1.7), visible as a finite intercept of the asymptotic straight line on the  $\sqrt{t}$ -axis in the inset in Fig. 1.

The paper is organized as follows: After summarizing in Sec. II the idea of the continuous label variable method and some of its results, we apply it to the calculation of the two-particle displacement correlation in

Sec. III. Strictly speaking, what we present in Sec. III is not  $\langle R_i R_j \rangle$  itself but its continuum equivalent, calculated theoretically for the longtime regime. Subsequently, in Sec. IV we demonstrate a systematic and FDT-preserving derivation of an MCT-like equation in the Lagrangian description. The “Lagrangian” MCT equation provides us with the finite-time correction to MSD and the two-particle displacement correlation. With this finite-time correction taken into account, two different forms of four-point correlation functions are calculated in Sec. V: one is  $X_R(\vec{d}, t)$  and the other is  $\chi_4^S(t)$ . Section VI is allotted for discussion and concluding remarks.

## II. CONTINUUM THEORY OF SINGLE-FILE DIFFUSION

Let us begin with summarizing our previous results on MSD for SFD [24]. By “continuum theory” we mean that the theory is formulated in terms of some hydrodynamic quantity such as the density  $\rho$ , rather than direct treatment of the particles. Our idea consists in adoption of the continuous label variable  $\xi$ , which we take instead of the position  $x$  as the independent variable, and we also change the dependent variable from the density  $\rho(x, t)$  to the fluctuation of the particle interval, denoting it with  $\psi(\xi, t)$ . On the basis of the correlation of  $\psi$  calculated for the longtime regime, we can re-derive Eq. (1.7).

Since our label variable method is intended as a reformulation of MCT, we start from essentially the same Langevin equation as in field-theoretical formulation of MCT for dense colloidal suspension [38]. The Langevin equation, derived from Eq. (1.5) for the density  $\rho(x, t) = \sum_j \rho_j$  with  $\rho_j = \delta(x - X_j(t))$  and its flux  $Q = \sum_j \rho_j \dot{X}_j$ , is given as follows:

$$\partial_t \rho + \partial_x Q = 0, \quad (2.1a)$$

$$Q = -D \left( \partial_x \rho + \frac{\rho}{k_B T} \partial_x U \right) + \sum_j \rho_j(x, t) f_j(t), \quad (2.1b)$$

$$U = U[\rho](x) = \int dx' V(x - x') \rho(x'). \quad (2.1c)$$

By eliminating  $Q$  and introducing

$$f_\rho(x, t) = -\partial_x \sum_j \rho_j(x, t) f_j(t),$$

we write down the equation for  $\rho(x, t)$  as

$$\partial_t \rho(x, t) = D \partial_x \left( \partial_x \rho + \frac{\rho}{k_B T} \partial_x U \right) + f_\rho(x, t) \quad (2.2)$$

with  $\partial_x U = \partial_x U[\rho](x)$  and

$$\langle f_\rho(x, t) f_\rho(x', t') \rangle = 2D \partial_x \partial_{x'} \rho(x, t) \delta(x - x') \delta(t - t'). \quad (2.3)$$

Note the presence of  $\rho(x, t)$  on the right-hand side of Eq. (2.3): the noise is multiplicative [39].

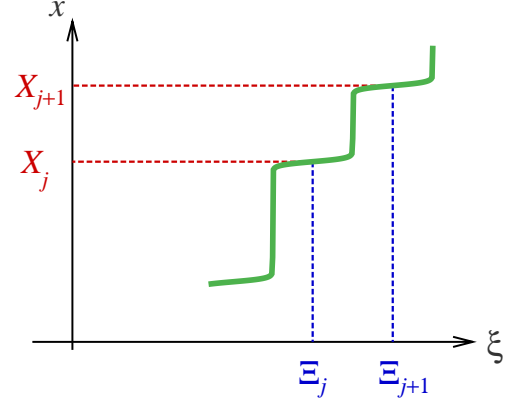


FIG. 2: (Color online) A schematic view of the mapping from  $\xi$  to  $x$ , given by inverting the function  $\xi = \xi(x, t)$  in Eq. (2.6), with  $t$  fixed arbitrarily. The label and the position of the  $j$ -th particle is denoted by  $\Xi_j$  and  $X_j$ , respectively.

As the particles have excluded volume effect and therefore cannot overlap, the barrier expressed by  $V$  must be infinitely high. In the one-dimensional system, this barrier acts as a topological constraint, or the “no overtaking” rule in plain words, which keeps the order of the particles. In MCT, however,  $V$  is replaced with a finite effective potential, either explicitly by hand (in the diagrammatic formalism) or implicitly by the projection operator (in the Mori-Zwanzig formalism). As a result, MCT cannot incorporate the “no overtaking” effect of  $V$  properly. An asymptotic analysis of one-dimensional MCT for longtime limit gives the normal diffusion, contradicting to Eq. (1.7) [9, 28].

When Miyazaki gave a talk on SFD [28], the present authors were nursing an idea of importing the concept of Lagrangian correlation from the theory of fluid turbulence [30–32] into the studies of glassy systems, and this idea was soon noticed to be applicable to SFD. The idea consists in adoption of the continuous label variable, which we denote with  $\xi$ .

Though it is popular in continuum mechanics to take the initial position of each material element to label it, here we define  $\xi$  in a different way, avoiding to trace the whole history of the system back to the initial configuration. We construct the label function  $\xi = \xi(x, t)$  so as to satisfy the following three requirements:

1. The label should satisfy the convective equation
$$(\rho \partial_t + Q \partial_x) \xi(x, t) = 0. \quad (2.4)$$
2. The label should be related to the snapshot of  $\rho$  and  $Q$  in such a way that the continuity equation (2.1a) is satisfied.
3. The function needs to be invertible, in the sense that a mapping from  $(\xi, t)$  to  $x = x(\xi, t)$  should exist.

To satisfy the second requirement, we utilize the fact that Poincaré's lemma [40] is applicable to the continuity equation (2.1a), which guarantees the existence of  $\xi$  such that

$$\partial_x \xi(x, t) = \rho, \quad \partial_t \xi(x, t) = -Q; \quad (2.5)$$

in fact, a solution to Eq. (2.5) is explicitly given by

$$\xi = \xi(x, t) = \int_{X_0(t)}^x \rho(x', t) dx' + \text{const.} \quad (2.6)$$

Then it is straightforward to verify that all the three requirements are satisfied. To be precise, since  $\rho$  consists of a sum of delta functions, the integral in Eq. (2.6) gives a multiple step function (see Fig. 2), which needs to be slightly smoothed to justify the single-valuedness and the invertibility. Although this smoothing could be interpreted physically as a consequence of coarse-graining, here we refrain from involving ourselves with such a delicate matter and regard the smoothing simply as a mathematical regularization. We define  $\Xi_j = \xi(X_j(t), t)$  for  $j \in \mathbb{Z}$ , taking it for granted that the particles are numbered consecutively; then, with the smoothing and the integral constant tuned appropriately, we have  $\Xi_j = j$ .

Using the label variable  $\xi$  as the spatial coordinate, now we rewrite the Langevin eq. (2.1). The chain rule for the differential operators gives

$$\partial_x = \frac{\partial \xi}{\partial x} \partial_\xi = \rho \partial_\xi, \quad (\partial_t \cdot)_x = (\partial_t \cdot)_\xi - Q \partial_\xi.$$

As a kinematic relation that replaces Eq. (2.1a), from the identity  $\partial_t \partial_\xi x = \partial_\xi \partial_t x$  we find

$$\partial_t \left[ \frac{1}{\rho(\xi, t)} \right] = \partial_\xi \left( \frac{Q}{\rho} \right). \quad (2.7)$$

Then, rewriting Eq. (2.1b) with  $\partial_\xi$  and substituting it into Eq. (2.7), we obtain

$$\begin{aligned} \partial_t \left[ \frac{1}{\rho(\xi, t)} \right] &= -D \partial_\xi \left( \partial_\xi \rho + \frac{\rho}{k_B T} \partial_\xi U \right) \\ &\quad + \partial_\xi \sum_j \delta(\xi - \Xi_j) f_j(t) \\ &= -D \partial_\xi [\partial_\xi \rho + 2 \sinh(\rho \sigma \partial_\xi) \rho] + f_L(\xi, t), \end{aligned} \quad (2.8)$$

where  $V$  is replaced with the effective potential as before, and  $f_L$  satisfies

$$\langle f_L(\xi, t) f_L(\xi', t') \rangle = 2D \partial_\xi \partial_{\xi'} \sum_i \delta(\xi - \Xi_i) \delta(\xi - \xi') \delta(t - t'). \quad (2.9)$$

Having changed the independent variables from  $(x, t)$  to  $(\xi, t)$ , we change the dependent variable as well. Introducing the fluctuation of the particle interval,

$$\psi = \psi(\xi, t) = \frac{\rho_0}{\rho(\xi, t)} - 1, \quad (2.10)$$

and its Fourier modes

$$\check{\psi}(k, t) = \frac{1}{N} \int d\xi e^{ik\xi} \psi(\xi, t) \quad \left( \frac{k}{2\pi/N} \in \mathbb{Z} \right), \quad (2.11)$$

we rewrite Eq. (2.8) in the form

$$\begin{aligned} \partial_t \check{\psi}(k, t) &= -D_* k^2 \left( 1 + \frac{2 \sin \rho_0 \sigma k}{k} \right) \check{\psi}(k, t) \\ &\quad + \sum_{k+p+q=0} \mathcal{V}_k^{pq} \check{\psi}(-p, t) \check{\psi}(-q, t) + O(\check{\psi}^3) \\ &\quad + \rho_0 \check{f}_L(k, t) \end{aligned} \quad (2.12)$$

with  $D_* = \rho_0^2 D$  and

$$\begin{aligned} \mathcal{V}_k^{pq} &= D_* k^2 \left( 1 + \frac{k}{pq} \sin \rho_0 \sigma k + \frac{p}{kq} \sin \rho_0 \sigma p + \frac{q}{kp} \sin \rho_0 \sigma q \right). \end{aligned} \quad (2.13)$$

As for the statistics of the random force term, Eq. (2.9) is re-expressed as

$$\rho_0^2 \langle \check{f}_L(k, t) \check{f}_L(-k', t') \rangle = \frac{2D_*}{N} k^2 \delta_{kk'} \delta(t - t'); \quad (2.14)$$

see Endnote [41]. We also note that the linearization of Eq. (2.12) coincides with the one-dimensional version of Edwards–Wilkinson equation [42, 43].

To calculate MSD, we developed a formula for it in terms of the correlation  $\langle \psi(\xi, t) \psi(\xi', 0) \rangle$ , or its Fourier transform  $\langle \check{\psi}(k, t) \check{\psi}(-k', 0) \rangle$ . In Fourier representation, the formula reads as follows:

$$\langle R^2 \rangle = \frac{L^4}{\pi N^2} \int_{-\infty}^{\infty} \frac{\check{C}(k, 0) - \check{C}(k, t)}{k^2} dk \quad (2.15)$$

where [44]

$$\check{C}(k, t) = \frac{N}{L^2} \langle \check{\psi}(k, t) \check{\psi}(-k, 0) \rangle. \quad (2.16)$$

In Sec. III, this formula will be re-derived as a special case of Eq. (3.2). We note that Eq. (2.15) may be regarded as a refinement of the approximate formula by Alexander and Pincus [19],

$$\langle R^2 \rangle \simeq \text{const.} \times \int_{-\infty}^{\infty} \frac{F(q, 0) - F(q, t)}{q^2} dq, \quad (2.17)$$

and therefore Eq. (2.15) may be referred to as the modified Alexander–Pincus formula. In the linear (Edwards–Wilkinson) case, a  $n_d$ -dimensional version of Eq. (2.17) has appeared in the literature [5, 45, 46]; we will discuss it later in Sec. VI, calling attention to some delicate points about the extension to the  $n_d$ -dimensional liquid dynamics.

Once the formula (2.15) is derived, all depends on the knowledge of  $\check{C}$ . In particular, the long-time behavior of



MSD is found by linear analysis of Eq. (2.12). From the linearized equation, the correlation  $\check{C}$  is calculated as

$$\check{C}(k, t) = \frac{S}{L^2} e^{-(D_*/S)k^2 t} \quad (2.18)$$

with the aid of Eq. (2.14). Substituting Eq. (2.18) into Eq. (2.15), we can successfully re-derive the subdiffusion law in Eq. (1.7). A refinement of Eq. (2.18), including the effect of the nonlinear term, will be discussed later in Sec. IV.

### III. FOUR-POINT CORRELATION

#### A. Cooperative motion in SFD

The slow dynamics in SFD is associated with collective motion of the particles. This collective motion, obtained by numerical integration of Eq. (1.5), is depicted in Fig. 3. In the numerical calculations (see Appendix A for details), after the system has reached the thermal equilibrium, we choose some instance as  $t = 0$  and record the “initial” position of each particle, say,  $X_i(0)$ . To produce Fig. 3(a), at  $t = 2^n \times 10\sigma^2/D$  (with  $n = 1, 2, \dots$ ) we measured the displacement  $R_i(t) = X_i(t) - X_i(0)$  for each  $i$ . If  $R_i(t) > 5\sigma$ , we mark the position of the particle with a circle ( $\circ$ ); if  $R_i < -5\sigma$ , we mark it with a cross ( $\times$ ). As the time difference  $t$  increases, a string of the same kind of symbol is formed, expressing a cluster of particles in cooperative motion. While Fig. 3(a) presents a close-up for a relatively limited time span, a long shot up to  $t = 10^6\sigma^2/D$  is shown as Fig. 3(b). Formation of large clusters in cooperative motion is visible. By the time difference  $t = 10^6\sigma^2/D$ , a typical cluster reaches the size of several hundred particles, occupying a length on the order of  $10^3\sigma$  (as each particle is assigned a space of  $1/\rho_0 = 4\sigma$ ).

Quantitative description of this collective motion requires some four-point correlation functions, such as those used for the analysis of dynamical heterogeneity in glassy systems. In regard to SFD, it seems especially natural to consider the four-point correlation to deal with the topological constraint of the “no passing” rule, as the requirement that two world lines should not intersect involves four points in the space-time, namely  $X_i(0)$ ,  $X_j(0)$ ,  $X_i(t)$ , and  $X_j(t)$ . This is why Miyazaki & Yethiraj [16] needed to calculate a four-point correlation  $[G(1, 2; 3, 4)]$  in their notation] to study the entanglements of rod polymers within the framework of liquid state theory.

Here we demonstrate that the label variable method is also capable of calculating a kind of four-point correlation, in the form of two-particle displacement correlation. Though it was originally presented as  $\langle R_i R_j \rangle$  in Eq. (1.8), there is no trouble in replacing the particle numbering with the label variable. Then, our task is derivation of a formula to calculate  $\langle R(\xi, t) R(\xi', t) \rangle$  with

$R(\xi, t) = x(\xi, t) - x(\xi, 0)$ , which will be shown in the next subsection.

#### B. Two-Particle Displacement Correlation

Aiming for an analytical expression for  $\langle R(\xi, t) R(\xi', t) \rangle$  in SFD, let us extend Eq. (2.15) so that we can calculate  $\langle R(\xi, t) R(\xi', t) \rangle$  from the correlation  $\check{C}$  defined by Eq. (2.16). We start with noticing that  $Q/\rho$  stands for the velocity, whose integral in regard to  $t$  gives the displacement of the particle labelled with  $\xi$ :

$$R(\xi, t) = \int_0^t dt' \frac{Q(\xi, t')}{\rho(\xi, t')}.$$

Into this equation we substitute  $Q/\rho = \partial_\xi^{-1} \partial_t (1/\rho)$ , obtained from Eq. (2.7) upon integration over  $\xi$ , to find

$$\begin{aligned} R(\xi, t) &= \partial_\xi^{-1} \left( \frac{1 + \psi}{\rho_0} \right) \Big|_0^t \\ &= \frac{1}{\rho_0} \sum_k \frac{e^{-ik\xi}}{-ik} [\check{\psi}(k, t) - \check{\psi}(k, 0)]. \end{aligned} \quad (3.1)$$

Subsequently, we multiply Eq. (3.1) by its duplicate with  $(\xi, k)$  changed to  $(\xi', -k')$ , and take the statistical average. The double summation on the right-hand side reduces to the single one, if we assume that the contribution from the terms with  $k \neq k'$  vanishes. This is true in the linear case, and also seems to be justifiable for nonlinear cases within the framework of the direct-interaction approximation (explained later). Thus we obtain a formula allowing us to calculate 2pDC from  $\langle \psi \psi \rangle$ :

$$\begin{aligned} \langle R(\xi, t) R(\xi', t) \rangle &= \frac{L^4}{\pi N^2} \int_{-\infty}^{\infty} dk e^{-ik(\xi - \xi')} \frac{\check{C}(k, 0) - \check{C}(k, t)}{k^2}, \end{aligned} \quad (3.2)$$

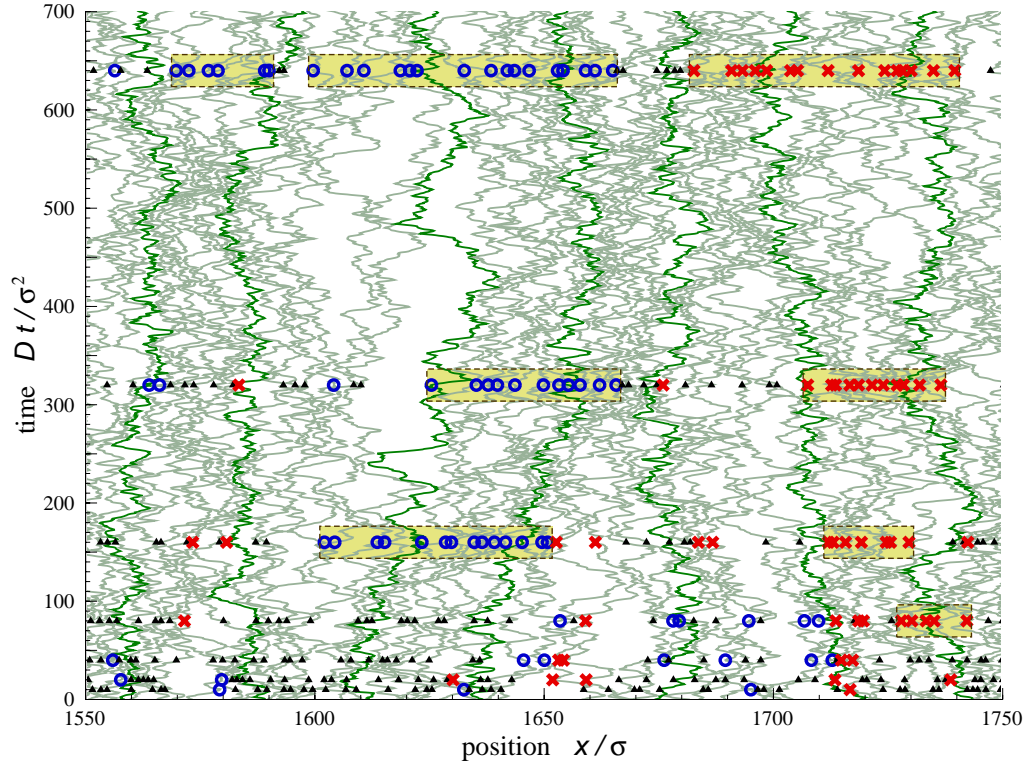
with  $\check{C}(k, t)$  defined by Eq. (2.16). Note that Eq. (3.2) includes the modified Alexander–Pincus formula (2.15) as a special case with  $\xi = \xi'$ , as it ought to be. In this sense, the formula (3.2) could be referred to as the *extended Alexander–Pincus formula*. We emphasize that Eq. (3.2) does not rely on smallness of deformation, nor it requires such kind of approximation at all, as long as the Lagrangian description is strictly followed.

#### C. Calculation of 2pDC: linear approximation

For  $\check{C}$  in Eq. (2.18) calculated from the linear approximation of Eq. (2.12), the extended Alexander–Pincus formula (3.2) gives

$$\begin{aligned} \langle R(\xi, t) R(\xi', t) \rangle &= \frac{2S}{\rho_0} \sqrt{\frac{D_c t}{\pi}} \exp \left[ -\frac{(\xi - \xi')^2}{4\rho_0^2 D_c t} \right] - \frac{S}{\rho_0^2} |\xi - \xi'| \operatorname{erfc} \frac{|\xi - \xi'|}{2\rho_0 \sqrt{D_c t}}. \end{aligned} \quad (3.3)$$

(a)



(b)

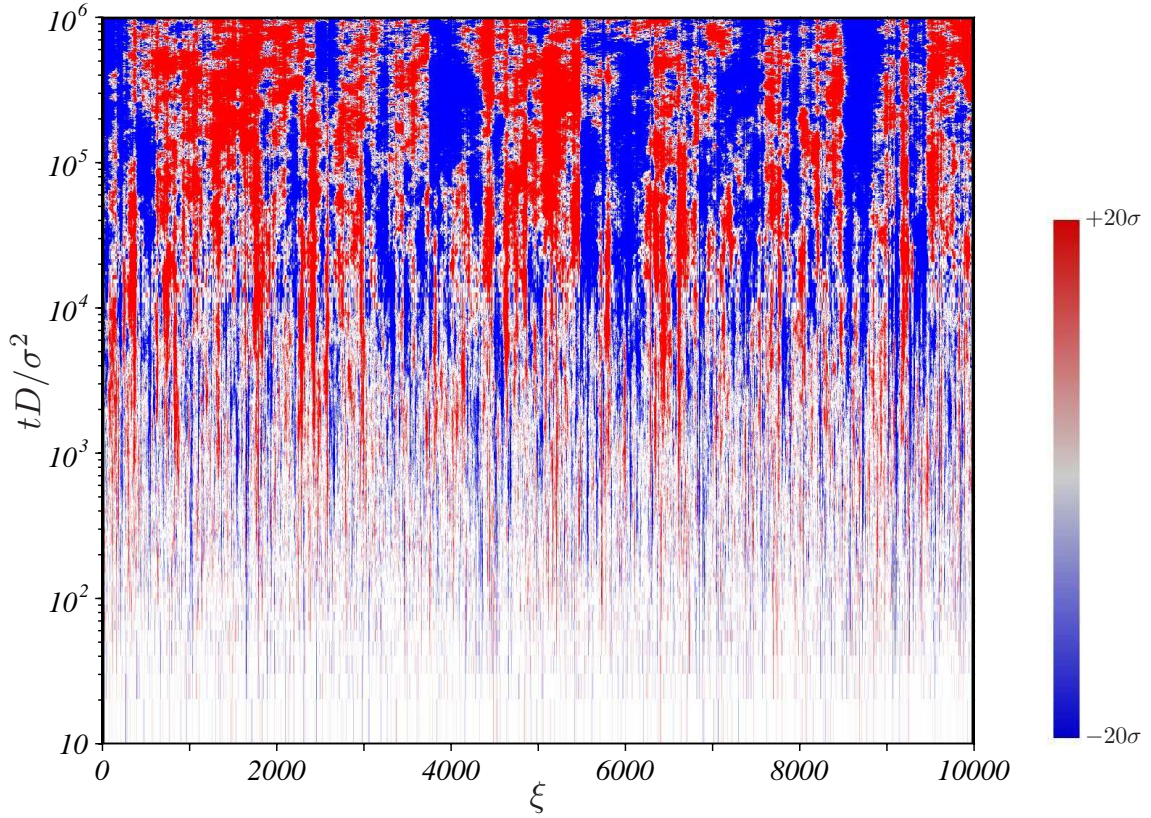


FIG. 3: (Color online) Clusters in cooperative motion visualized in space-time diagrams of particles in SFD, calculated for  $\rho_0 = N/L = 0.25 \sigma^{-1}$ . (a) Worldlines of particles in the  $(x, t)$ -plane. The symbols  $\bigcirc$  and  $\times$  mark particles displaced (by more than  $5\sigma$ ) rightward and leftward, respectively. The unmoving particles are indicated with small triangles. Each cluster in cooperative motion, involving 5 particles at least, is highlighted in a box. (b) The displacement  $R$  depicted in gray scale (blue-to-red scale online) as a function of  $\xi$  and  $t$ . Unmoving particles are shown in white.

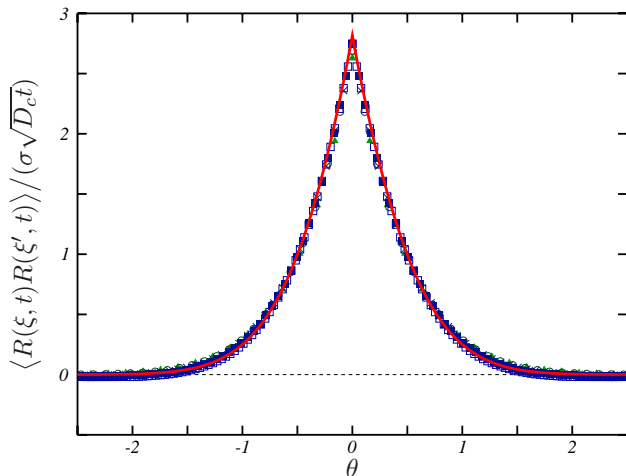


FIG. 4: (Color online) Comparison of Eq. (3.3) with the computed 2pDC in the same system as in Fig. 1 ( $N = 2^{15} = 32768$ ,  $\rho_0 = N/L = 0.25 \sigma^{-1}$ ). The solid (red) line shows the self-similar solution in Eq. (3.3), while the simulation data are plotted with symbols: solid triangles (▲) for  $t = 100 \sigma^2/D$ , open circles (○) for  $t = 200 \sigma^2/D$ , crosses (×) for  $t = 400 \sigma^2/D$ , open squares (□) for  $t = 800 \sigma^2/D$ , and solid squares (■) for  $t = 1600 \sigma^2/D$ .

This is expressible in terms of a similarity variable

$$\theta = \frac{\xi - \xi'}{2\rho_0\sqrt{D_c t}} \quad (3.4)$$

as

$$\frac{\langle R(\xi, t)R(\xi', t) \rangle}{\sigma\sqrt{D_c t}} = \frac{2S}{\rho_0\sigma} \left( \frac{e^{-\theta^2}}{\sqrt{\pi}} - |\theta| \operatorname{erfc}|\theta| \right) = \varphi(\theta). \quad (3.5)$$

From this similarity solution we can read the size  $\lambda$  of a cluster in a cooperative motion,

$$\lambda = \lambda(t) = 2\sqrt{D_c t}. \quad (3.6)$$

We have already seen such clusters in Fig. 3, though care should be taken in regard to the difference that Eq. (3.6) is a statistical law while Figs. 3(a) and (b) present a single run, and only a small portion of it is shown in Fig. 3(a).

Equation (3.3) is compared with statistical results of particle simulations in Fig. 4. Except for the transient behavior slightly visible for  $t = 100 \sigma^2/D$ , all of the simulation results are consistent with Eq. (3.3). The transient behavior can be studied by taking the nonlinear terms in Eq. (2.12) into account, which will be discussed in the next section.

The variable for the horizontal axis of Fig. 4 requires some consideration. As a quantity corresponding to  $\xi - \xi'$ , here we have taken the distance in the label numbering, say,  $|i - j|$  between the  $i$ -th and  $j$ -th particle. Though adequate in the present case, this is not convenient for extensions to multidimensional cases [12, 37], because the result may depend on the way of numbering. A rea-

sonable alternative in the particle simulation is the initial distance such as  $X_i(0) - X_j(0)$ , which can be compared with the theoretical prediction by assuming that  $(\xi - \xi')/\rho_0$  corresponds to  $X_i(0) - X_j(0)$  after statistical averaging. Numerical calculations show that this is indeed valid as far as the longtime behavior is concerned, but transiently there are additional modifications due to triple correlations such as  $\langle \check{\psi}(-p, 0)\check{\psi}(-q, 0)\check{\psi}(-k, t) \rangle$ . Before discussing these modifications, let us develop nonlinear closure theory for  $\check{C}$ , which gives the triple correlation as a byproduct.

#### IV. NONLINEAR THEORY FOR FINITE-TIME EFFECTS

##### A. Inclusion of nonlinearity: DIA for SFD

The expression for 2pDC in Eq. (3.3) is based on the linear approximation to Eq. (2.12), which is only asymptotically valid for sufficiently long time. For finite values of  $t$ , there should be a correction to Eq. (3.3) describing the transient behaviors of 2pDC and MSD; to find this correction, now we develop a nonlinear closure theory for the correlation  $\check{C}$ .

In short, what we present here and in the next subsection is a systematic derivation of MCT equation for  $\check{C}$ . Except for some minor (but important) differences, this is analogous to the attempt of a number of authors [39, 47, 48] who tried to re-derive MCT equation with the Martin-Siggia-Rose (MSR) formalism [49]. They were obstructed by the problem of inconsistency with FDT: this difficulty is inevitable for dense colloidal suspensions or supercooled liquids, as long as one uses the standard MSR formalism with the plain  $\hat{\rho}(\mathbf{k}, t)$  as the field variable [50–52]. Only some special classes of Langevin equations are free from this difficulty. Two such classes are known: one is the class of models whose nonlinearity comes from the gradient of the thermodynamic potential (entropy) alone, such as the  $p$ -spin model, referred to as “Class I” by Miyazaki & Reichman; and the other one (called “Class II”) is exemplified by liquid models with Gaussian approximation to the entropy [39, 48]. Fortunately, our equation for  $\check{\psi}$  belongs to Class I and therefore consistency with FDT is expected.

Let us return to the nonlinear Langevin equation (2.12) governing  $\check{\psi}$ , with the random force statistics in Eq. (2.14). The correlation  $\check{C}$  is then subject to an equation containing triple correlations:

$$\begin{aligned} & \left( \partial_t + \frac{D_*}{S} k^2 \right) \check{C}(k, t) \\ &= \frac{N}{L^2} \sum_{k+p+q=0} \mathcal{V}_k^{pq} \langle \check{\psi}(-p, t)\check{\psi}(-q, t)\check{\psi}(-k, 0) \rangle, \end{aligned}$$

with the  $O(\check{\psi}^3)$  term in Eq. (2.12) discarded. Note the absence of  $\langle \check{f}_L \check{\psi} \rangle$  on the right-hand side; this term vanishes because  $f_L$  is not multiplicative, which means that



$\langle \check{f}_L(k, t) \check{f}_L(-k', t') \rangle$  is independent of the  $\check{\psi}$ 's according to Eq. (2.14). To provide a closure to this equation, we apply the formalism of *direct-interaction approximation* (DIA) [29–32, 53]. The procedure of the calculation is essentially the same as that in Ref. [54] and is explained briefly in Appendix B. As a result, we obtain a set of equations:

$$\begin{aligned} \left( \partial_t + \frac{D_*}{S} k^2 \right) \check{C}(k, t) &= \int_{t_0}^t dt' M_G(k, t - t') \check{C}(k, |t'|) \\ &+ \int_{t_0}^0 dt' M_C(k, t - t') \bar{G}(-k, -t') \end{aligned} \quad (4.1)$$

$$\left( \partial_t + \frac{D_*}{S} k^2 \right) \bar{G}(k, t) = \int_0^t dt' M_G(k, t - t') \bar{G}(k, t') \quad (4.2)$$

for the correlation  $\check{C}$  and

$$\bar{G}(k, t - t') = \langle G(k, t; k, t') \rangle = \left\langle \frac{\delta \check{\psi}(k, t)}{\delta \check{\psi}(k, t')} \right\rangle,$$

with  $t_0 (< 0)$  denoting the time at which the “direct interactions” are switched off, and  $M_G$  and  $M_C$  are memory kernels given by

$$M_G(k, s) = \frac{4L^2}{N} \sum \mathcal{V}_k^{pq} \mathcal{V}_q^{pk} \check{C}(p, s) \bar{G}(-q, s), \quad (4.3)$$

$$M_C(k, s) = \frac{2L^2}{N} \sum (\mathcal{V}_k^{pq})^2 \check{C}(p, s) \check{C}(q, s). \quad (4.4)$$

Note that, in the present case, the propagator (Kraichnan’s response function)  $\bar{G}$  is essentially equivalent to the

response function to an externally applied probe force, because the random forcing term  $\rho_0 f_L$  in Eq. (2.12) is not multiplicative but additive.

In regard to the choice of  $t_0$ , we consider two possibilities. Choosing  $t_0 \rightarrow -0$  would admit a solution of the form  $\check{C}(t) = \bar{G}(t) \check{C}(0)$ , which corresponds to the “Class II” approximation; we do not take this choice, as this would require the Langevin equation to belong to Class I and II simultaneously, leading to a result that is either trivial or inconsistent with FDT. Instead, we take  $t_0 \rightarrow -\infty$ , so that Eqs. (4.1) and (4.2) become identical to the standard one-loop result of the MSR formalism [49].

## B. Label-based MCT equation for SFD

In principle, Eqs. (4.1) and (4.2) with the initial conditions

$$\check{C}(k, 0) = \frac{S(k)}{L^2}, \quad \bar{G}(k, 0) = 1$$

should suffice for determination of  $\check{C}$  and  $\bar{G}$ . However, as soon as we start to calculate them in this straightforward way, we find us confronted with difficulties. Since we have  $t_0 \rightarrow -\infty$ , the equations are acausal. Besides, the memory terms seem to suffer ultraviolet divergence. To elude these difficulties, we differentiate Eq. (4.1) in regard to  $t$  and add it to Eq. (4.2) multiplied by  $\alpha_0 k^2$  with some constant  $\alpha_0$ , to write an equation for  $\partial_t \check{C} + \alpha_0 k^2 \bar{G}$ :

$$\begin{aligned} \left( \partial_t + \frac{D_*}{S} k^2 \right) [\partial_t \check{C}(k, t) + \alpha_0 k^2 \bar{G}(k, t)] &= \int_0^t dt' M_G(k, t - t') [\partial_t \check{C}(k, t') + \alpha_0 k^2 \bar{G}(k, t')] \\ &+ \int_{t_0}^0 dt' \{ M_G(k, t - t') \partial_{t'} \check{C}(k, -t') - [\partial_{t'} M_C(k, t - t')] \bar{G}(-k, -t') \}. \end{aligned} \quad (4.5)$$

The second term on the right-hand side includes  $\mathcal{V}$ 's through the memory kernels, which we rewrite by substituting Eqs. (4.3) and (4.4). Subsequently, introducing  $W$  by  $\mathcal{V}_k^{pq} = D_* k^2 W_{kpq}$  and making use of the symmetry of  $W$  [see Eq. (2.13)], after some algebraic manipulation, we find

[the integrand in the 2nd term on RHS of Eq. (4.5)]

$$\begin{aligned} &= \frac{4L^2}{N} D_*^2 k^2 \sum W_{kpq}^2 [q^2 \bar{G}(-q, t - t') \partial_{t'} \check{C}(k, -t') - k^2 \bar{G}(k, -t') \partial_{t'} \check{C}(q, t - t')] \\ &= \frac{4L^2}{N} D_*^2 k^2 \sum W_{kpq}^2 \times \\ &\quad \{ q^2 \bar{G}(-q, t - t') [\partial_{t'} \check{C}(k, -t') - \alpha_0 k^2 \bar{G}(k, -t')] - k^2 \bar{G}(k, -t') [\partial_{t'} \check{C}(-q, t - t') - \alpha_0 k^2 \bar{G}(-q, t - t')] \}. \end{aligned}$$

Then Eq. (4.5) can be replaced with a simpler relation

$$\partial_t \check{C}(k) + \alpha_0 k^2 \bar{G}(k, t) = 0 \quad (\text{for } \forall k), \quad (4.6)$$

in the sense that both sides of Eq. (4.5) vanishes if Eq. (4.6) holds. The constant  $\alpha_0$  is determined to be

$\alpha_0 = D_*/L^2$  by the initial condition.

Taking notice of the property of Eq. (2.12) that the propagator  $\bar{G}$  is equivalent to the response to the probe force, we note that Eq. (4.6) states the fluctuation–dissipation theorem (FDT), which can be derived directly from the Langevin equation (2.12) through the distribution function [55–57]. In other words, FDT is *already included* in Eqs. (4.1) and (4.2). This inclusion is a remarkable feature of Eq. (2.12), or Eq. (2.8), if we compare it with an analogous calculation starting from the Fourier representation of the “Eulerian” equation (2.2), as opposed to the “Lagrangian” equation (2.8). In the “Eulerian” case, the step corresponding to the rearrangement of Eq. (4.5) turns out to be inconsistent with FDT [54]. This inconsistency is due to the hidden dependence of  $f_\rho(x, t)$  on  $\rho$  in its statistics in Eq. (2.3), known as the multiplicative noise [39], which makes the “Eulerian” equation intractable with DIA-like expansion. Contrastively, the statistics of  $f_L$  on the RHS of the “Lagrangian” equation (2.8) is given by Eq. (2.9) which is *independent* of  $\psi$ . This is why the DIA equations (4.1) and (4.2) successfully reproduce FDT.

Equation (4.6) allows us to eliminate  $\bar{G}$  from Eq. (4.1) and thereby elude the difficulties mentioned at the beginning of this subsection, as it implies

$$\bar{G}(k, t) = -\frac{1}{\alpha_0 k^2} \partial_t \check{C}(k, t),$$

from which we can show

$$M_G(k, s) = -\frac{1}{\alpha_0 k^2} \partial_s M_C(k, s).$$

Then we substitute it into Eq. (4.1), and the result reads

$$\begin{aligned} & \left( \partial_t + \frac{D_*}{S} k^2 \right) \check{C} \\ &= \frac{1}{\alpha_0 k^2} \left[ M_C(k, 0) \check{C} - \int_0^t dt' M_C(k, t-t') \partial_{t'} \check{C}(k, t') \right]. \end{aligned}$$

The source of the ultraviolet divergence is now isolated in  $M_C(k, 0)$ , which we should discard, as this term seems to have originated from an inappropriate treatment of the self-interaction in DIA [58]. Thus we arrive at the MCT equation:

$$\left( \partial_t + \frac{D_*}{S} k^2 \right) \check{C}(k, t) = - \int_0^t dt' M(k, t-t') \partial_{t'} \check{C}(k, t') \quad (4.7)$$

where

$$\begin{aligned} M(k, s) &= \frac{M_C(k, s)}{\alpha_0 k^2} \\ &= \frac{2L^4}{N} D_* k^2 \sum_{p+q=k} W_{pqk}^2 \check{C}(p, s) \check{C}(q, s). \end{aligned} \quad (4.8)$$

### C. Solution to MCT equation

Now the finite-time correction to Eq. (3.3) for 2pDC is within our reach: all we need to do is to solve Eq. (4.7) and substitute the solution  $\check{C}$  into the extended Alexander–Pincus formula (3.2). Although one may switch to numerical remedy, here we prefer to stick to the fully analytical calculation, which is possible by assuming the dilute limit ( $\rho_0 \sigma \rightarrow +0$ ;  $S = 1$ ,  $D_c = D$ ). This does not trivialize the problem, because nonlinearity still exists due to

$$\frac{1}{1+\psi} = 1 - \psi + \psi^2 - \dots$$

and therefore the RHS of the MCT equation (4.7) does not vanish. Let us evaluate it using the linear solution Eq. (2.18) as the zeroth approximation valid for  $t \rightarrow +\infty$ , which now reads  $\check{C}(k, t) \simeq L^{-2} e^{-D_* k^2 t}$  as  $S = 1$ .

To start with, we calculate  $M(k, s)$  by substituting the approximate solution into Eq. (4.8). Parametrizing the variables in the summation as  $(p, q) = (k/2 + m, k/2 - m)$  and denoting the wave number interval with  $\Delta m = 2\pi/N$ , we find

$$M(k, s) = \frac{D_* k^2}{\pi} \sum_m \exp \left[ -D_* \left( \frac{1}{2} k^2 + 2m^2 \right) s \right] \Delta m.$$

The summation is then replaced with an integral, which readily yields

$$M(k, s) = \frac{D_* k^2}{\sqrt{2\pi D_* s}} e^{-\frac{1}{2} D_* k^2 s}$$

and therefore

$$\begin{aligned} & [\text{RHS of Eq. (4.7)}] \\ &= \frac{D_*^2 k^4}{L^2} e^{-D_* k^2 t} \int_0^t \frac{dt'}{\sqrt{2\pi D_* (t-t')}} e^{-\frac{1}{2} D_* k^2 (t-t')}. \end{aligned} \quad (4.9)$$

Though the integral in Eq. (4.9) can be evaluated rigorously in terms of the error function with an imaginary argument, it is more convenient to evaluate it by expanding the integrand in powers of  $t' - t$ , as the largest contribution to the integral comes from the vicinity of  $t' = t$ . Thus we find

$$\begin{aligned} & [\text{RHS of Eq. (4.7)}] \\ &= \frac{D_*^2 k^4}{L^2} e^{-D_* k^2 t} \left[ \sqrt{\frac{2}{\pi}} D_* t + \frac{k^2}{3} \sqrt{\frac{(D_* t)^3}{2\pi}} + \dots \right], \end{aligned}$$

which allows us to integrate Eq. (4.7) as

$$\begin{aligned} \check{C} &= \frac{1}{L^2} e^{-D_* k^2 t} \times \\ & \left[ 1 + \frac{2}{3} \sqrt{\frac{2}{\pi}} k^4 (D_* t)^{3/2} + \frac{2}{15\sqrt{2\pi}} k^6 (D_* t)^{5/2} + \dots \right]. \end{aligned} \quad (4.10)$$

It should be possible, at least in principle, to substitute Eq. (4.10) into Eq. (4.8) and the RHS of Eq. (4.7) for the second approximation, but for the present let us content ourselves with this first approximation to go ahead.

#### D. Effects of the nonlinear term on transient behaviors of MSD and 2pDC

Since  $\tilde{C}$  is now available in Eq. (4.10) as a result of nonlinear closure theory, we can evaluate  $\langle R(\xi, t)R(\xi', t) \rangle$

$$\begin{aligned} \langle R(\xi, t)R(\xi', t) \rangle &= \frac{2}{\rho_0} \sqrt{\frac{Dt}{\pi}} \exp \left[ -\frac{(\xi - \xi')^2}{4\rho_0^2 Dt} \right] - \frac{|\xi - \xi'|}{\rho_0^2} \operatorname{erfc} \frac{|\xi - \xi'|}{2\rho_0 \sqrt{Dt}} - \frac{\sqrt{2}}{3\pi} \rho_0^{-2} \left[ 1 - \frac{(\xi - \xi')^2}{2\rho_0^2 Dt} \right] \exp \left[ -\frac{(\xi - \xi')^2}{4\rho_0^2 Dt} \right] \\ &= \sigma \sqrt{Dt} \varphi(\theta) - \frac{\sqrt{2}}{3\pi} \rho_0^{-2} (1 - 2\theta^2) e^{-\theta^2} \end{aligned} \quad (4.11)$$

where  $\theta = (\xi - \xi')/(2\rho_0 \sqrt{Dt})$  and the function  $\varphi$  is defined in Eq. (3.5) with  $S = 1$ . As a special case for  $\xi = \xi'$ , Eq. (4.11) gives correction to  $\langle R^2 \rangle \propto \sqrt{t}$ :

$$\langle R^2 \rangle = \frac{2}{\rho_0} \sqrt{\frac{Dt}{\pi}} - \frac{\sqrt{2}}{3\pi} \rho_0^{-2}. \quad (4.12)$$

The first term reproduces Eq. (1.7) with  $S = 1$ , while the second term gives a correction to it. The contribution from the higher-order terms in Eq. (4.10) slightly enlarges the coefficient of the correction term, but the form of Eq. (4.12) itself is not affected.

Without the second term in Eq. (4.12), plotting  $\langle R^2 \rangle$  against  $\sqrt{t}$  would yield a graph of a straight line passing through the origin. In actuality, the second term in Eq. (4.12) shifts the asymptotic straight line, making a positive intercept on the  $\sqrt{t}$ -axis and a negative intercept on the  $\langle R^2 \rangle$ -axis. These intercepts are already visible in the inset of Fig. 1, and also in Fig. 5 (a plot analogous to Fig. 1 but with the axes rescaled, as we explain below). The presence of the correction itself is probably not surprising, because the short-time diffusion should behave as  $\langle R^2 \rangle \propto Dt$  before the collisions begin to take effect; it is more noteworthy that, since this single-particle behavior plays the role of the “mode-coupling” in the Fourier representation, the description of the transient behavior requires a nonlinear theory such as MCT.

The prediction of the nonlinear theory in Eq. (4.12), including its dependence on the density  $\rho_0$ , is compared with the computed MSD in Fig. 5. As the quantitative comparison requires us to take into account the effects of the finite density, we revived  $S = S(0)$  in the first term of Eq. (4.12), and plotted  $\rho_0^2 \langle R^2 \rangle$  against  $S(0)\rho_0 \sqrt{D_c t}$ . The MSD computed for three different values of density ( $\rho_0 \sigma = 1/4, 1/8$ , and  $1/16$ ; see the inset) seem to collapse into a single curve whose asymptote is the straight line

using the formula (3.2). The procedure is analogous to that for the derivation of Eq. (3.3) from the linear solution in Eq. (2.18).

If we take into account the term of order  $(D_* t)^{3/2}$  and ignore that of order  $(D_* t)^{5/2}$  in Eq. (4.10), by substituting Eq. (4.10) into the formula (3.2) we obtain

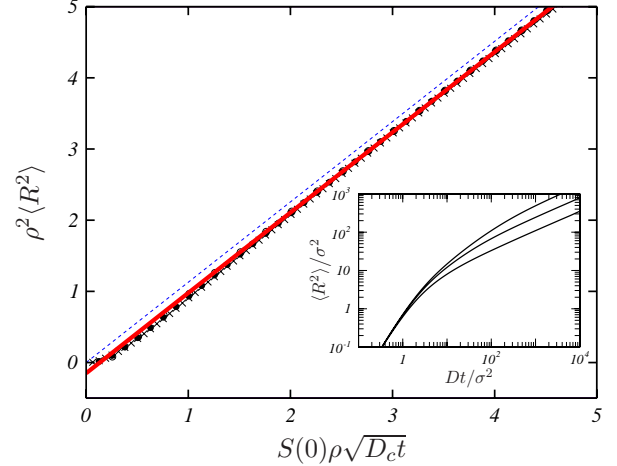


FIG. 5: (Color online) Comparison of Eq. (4.12) with numerical data, by means of rescaled plotting of MSD versus time for three different values of the density:  $\rho_0 = N/L = (1/4)\sigma^{-1}$ ,  $(1/8)\sigma^{-1}$ , and  $(1/16)\sigma^{-1}$ . The number of the particles is fixed at  $N = 2^{15} = 32768$ . The solid line represents the prediction of the nonlinear theory in Eq. (4.12), which is compared with Kollmann’s law (1.7) in the dotted line. The inset shows the same data without rescaling, using the simple nondimensionalization with  $\sigma^2$  and  $\sigma^2/D$ .

given by Eq. (4.12). Improvement of Eq. (4.12) accounting for the small deviation from the straight line will be performable with a careful numerical calculation of the MCT equation, which will be reported elsewhere.

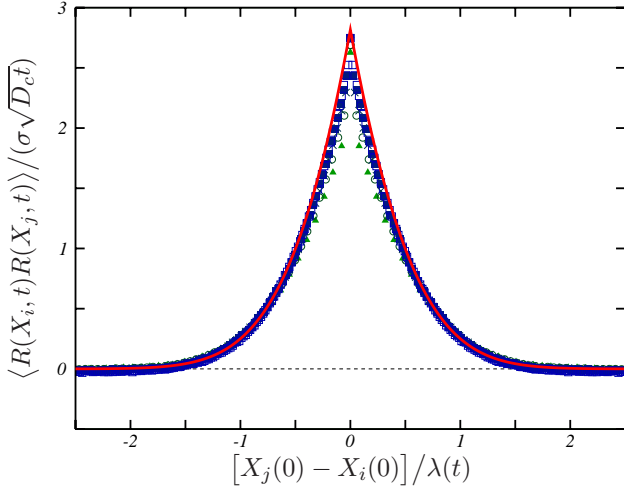


FIG. 6: (Color online) Eq. (3.3) compared with simulation data (with the same  $N$  and  $\rho_0$  as in Figs. 1 and 4), on the basis of the initial distance  $X_j(0) - X_i(0)$  instead of the particle numbering. The solid (red) line shows the theoretical prediction for  $t \rightarrow +\infty$  by Eq. (3.3), while the simulation data are plotted with the same symbols as in Fig. 4.

## V. OTHER FORMS OF FOUR-POINT CORRELATION DERIVED FROM 2PDC

### A. Behavior of 2pDC as a function of the initial distance

As we have already shown in Fig. 4, the theoretical prediction for  $\langle R(\xi, t)R(\xi', t) \rangle$  is almost perfectly consistent with numerical calculation. However, taking the label distance  $\xi - \xi'$  or  $\theta = (\xi - \xi')/[\rho_0\lambda(t)]$  for the horizontal axis of the graph is sometimes inconvenient, for example, when we try to compare the result with two-dimensional or three-dimensional numerical calculations. For this purpose, it may be more convenient to re-express the result as a function of the initial distance,  $X_j(0) - X_i(0)$ , and plot the two-particle displacement correlation against  $[X_j(0) - X_i(0)]/\lambda(t)$ . Such a graph is shown in Fig. 6. The analytic curve in Fig. 6 is drawn by simply equating  $[X_j(0) - X_i(0)]/\lambda(t)$  with  $\theta$  in Eq. (3.5). This seems to be valid for  $t \rightarrow +\infty$ , but a considerable discrepancy is seen for shorter times.

Although  $X_j(0) - X_i(0)$  and  $(\Xi_j - \Xi_i)/\rho_0$  are equal on the average, generally they are different, as is evident from the relation

$$X_j(0) - X_i(0) = \int_{\Xi_i}^{\Xi_j} \frac{1 + \psi(\xi, 0)}{\rho_0} d\xi. \quad (5.1)$$

This difference is responsible for the discrepancy in Fig. 6 for finite  $t$ . Taking this difference into account, we can evaluate 2pDC theoretically as a function of the initial distance. Although its complete evaluation is out of the scope of the present paper, as it seems to involve wavenumber integrals that are difficult to perform ana-

lytically, we can outline the procedure of the calculation at least.

With the value of the initial distance denoted with  $\tilde{d}$ , the function that gives 2pDC, which we denote with  $X_R(\tilde{d}, t)$ , is formally written as

$$X_R(\tilde{d}, t) = \left\langle \frac{1}{L} \iint \delta(x_1 - x_2 - \tilde{d}) R(\xi_1, t) R(\xi_2, t) dx_1 dx_2 \right\rangle \quad (5.2)$$

where

$$x_1 = x_1(\xi_1) = x(\xi_1, 0), \quad x_2 = x_2(\xi_2) = x(\xi_2, 0),$$

and therefore

$$x_2 - x_1 = \frac{1}{\rho_0} \left[ \xi_2 - \xi_1 + \int_{\xi_1}^{\xi_2} \psi(\xi, 0) d\xi \right].$$

Changing the variables of the integral in Eq. (5.2) from  $(x_1, x_2)$  to  $(\xi_1, \xi_2)$  with

$$dx_1 = \frac{1 + \psi(\xi_1, 0)}{\rho_0} d\xi_1, \quad dx_2 = \frac{1 + \psi(\xi_2, 0)}{\rho_0} d\xi_2,$$

and introducing the Fourier representation of the delta function,

$$\delta(\tilde{x}) = \frac{1}{L} \sum_q e^{-iq\tilde{x}} \quad \left( \frac{q}{2\pi/L} \in \mathbb{Z} \right),$$

we rewrite Eq. (5.2) as

$$X_R(\tilde{d}, t) = \sum_k e^{ik\rho_0\tilde{d}} \left\langle \tilde{R}(k, t) \tilde{R}(-k, t) \right\rangle \quad (5.3)$$

where  $k = q/\rho_0$  and

$$\begin{aligned} \tilde{R}(k, t) &= \frac{1}{L} \int_0^L e^{iqx} R(\xi(x, 0), t) dx \\ &= \frac{1}{N} \int_0^N \exp \left( ik \left[ \xi + \int_0^\xi \psi d\xi \right] \right) R(\xi, t) (1 + \psi) d\xi, \end{aligned} \quad (5.4)$$

with

$$\psi = \psi(\xi, 0), \quad \int_0^\xi \psi d\xi = \int_0^\xi \psi(\tilde{\xi}, 0) d\tilde{\xi}.$$

Then we express  $\psi$  in Eq. (5.4) with  $\check{\psi}$  in Eq. (2.11) and also substitute Eq. (3.1). After some rearrangement, we obtain

$$\begin{aligned} \tilde{R}(k, t) &= \frac{L}{N} \times \frac{\check{\psi}(k, t) - \check{\psi}(k, 0)}{-ik} \\ &+ \frac{L}{N} \sum_{p+p'=k} \frac{\check{\psi}(p, 0) [\check{\psi}(p', t) - \check{\psi}(p', 0)]}{ip} + O(\check{\psi}^3). \end{aligned} \quad (5.5)$$



Substituting Eq. (5.5) into Eq. (5.3) yields an expression of  $X_R(\tilde{\mathbf{d}}, t)$  that consists of two parts: the first part simply reproduces Eq. (3.2) with  $\xi - \xi'$  replaced with  $\rho_0 \tilde{\mathbf{d}}$ , and the second part involves triple correlations such as  $\langle \tilde{\psi}(-p, 0) \tilde{\psi}(-q, t) \tilde{\psi}(-k, t) \rangle$  with  $p + q + k = 0$ . These triple correlations can be calculated with DIA, and as a result, we obtain a correction term whose magnitude relative to the leading term decreases in proportion to  $t^{-1/2}$  for  $t \rightarrow +\infty$ . Detailed results of the calculation will be reported elsewhere.

We note that the definition of  $X_R$  in Eq. (5.2) is readily generalized to three-dimensional cases, as

$$\begin{aligned} \mathbf{X}(\tilde{\mathbf{d}}, t) &= \left\langle \frac{1}{L^3} \iint \delta^3(\mathbf{r}_{12} - \tilde{\mathbf{d}}) \mathbf{R}_1 \otimes \mathbf{R}_2 d^3 \mathbf{r}_1 d^3 \mathbf{r}_2 \right\rangle \\ &= \left\langle \frac{L^3}{N^2} \sum_i \sum_j \frac{\delta^3(\mathbf{r}_{ij} - \tilde{\mathbf{d}})}{g_2(\mathbf{r}_{ij})} \mathbf{R}_i \otimes \mathbf{R}_j \right\rangle, \end{aligned} \quad (5.6)$$

where  $\mathbf{r}_{ij} = \mathbf{r}_j - \mathbf{r}_i$ ,  $\mathbf{R}_i = \mathbf{R}(\boldsymbol{\xi}_i, t) = \mathbf{r}_i(t) - \mathbf{r}_i(0)$ , and

$$g_2(\mathbf{r}) = \frac{L^3}{N^2} \sum_{i'} \sum_{j'} \delta^3(\mathbf{r}_{j'} - \mathbf{r}_{i'} - \mathbf{r}).$$

This  $\mathbf{X}$  is similar to the quantity calculated by Donati *et al.* [37] ( $g_u$  in their notation), except for two main differences: in their  $g_u$ , the two-body density  $g_2$  is absent in the denominator, and a product of scalar displacements,  $|\mathbf{R}_i| |\mathbf{R}_j|$ , is used instead of  $\mathbf{R}_i \otimes \mathbf{R}_j$ . The presence or absence of  $g_2$  is not essential, though it indeed makes it difficult to define  $\mathbf{X}$  for small values of the initial distance,  $|\tilde{\mathbf{d}}| < \sigma$ , in which we are not interested. The other difference is crucial: the absolute value signs obstructs analytical evaluation of  $g_u$  even in the one-dimensional cases. Besides, the tensorial character of  $\mathbf{X}$  can provide a useful information on the geometry of the collective motion in the three-dimensional glassy systems. We will return to this point in Sec. VI, but before that, let us relate the one-dimensional 2pDC to  $\chi_4$ .

## B. Calculation of $\chi_4$ from 2pDC

With the knowledge of the displacement correlation  $\langle R(\xi, t) R(\xi', t) \rangle$  in Eq. (4.11), we can also calculate a one-dimensional version of a quantity which is commonly referred to as  $\chi_4(t)$ . To be precise, we consider the  $\mathcal{Q}$ -based  $\chi_4$  [13, 14], as opposed to other variants of  $\chi_4$  such as the  $F$ -based  $\chi_4$  [5, 59] defined through the fluctuation of the intermediate scattering function  $F$  or its self part. If we consult Glotzer *et al.* [13] and adapt their equations (4) and (5) for one-dimensional cases, we have

$$\mathcal{Q} = \sum_i \sum_j \bar{\delta}_a(X_j(t) - X_i(0)), \quad (5.7)$$

$$\chi_4(t) = \frac{L}{k_B T} \frac{\langle \mathcal{Q}^2 \rangle - \langle \mathcal{Q} \rangle^2}{N^2}. \quad (5.8)$$

This type of four-point correlation function has been studied by many authors [13, 14, 60–63] as an indicator of cooperative motion in glassy systems. To our knowledge, most of these studies are based on direct numerical simulations of particle systems and there are also experiments grounded on observation of particles, but analytical calculations are quite rare. What makes it difficult to calculate  $\chi_4$  analytically is that, in the usual formulation, the *four-point* correlation implies *four-body* correlation, i.e. it involves four bodies. More concretely, as  $\mathcal{Q}$  in Eq. (5.7) already contains double summation, calculation of  $\chi_4$  requires dealing with quadruple summation whose summand involves four particles simultaneously; this would be a hopeless task.

To facilitate calculation of four-point correlation, here we introduce two modifications to Eqs. (5.7) and (5.8). Firstly, we target on the “self part” ( $i = j$ ) of  $\mathcal{Q}$  and its contribution to  $\chi_4$ , denoting them as [64]

$$\mathcal{Q}_S = \sum_i \bar{\delta}_a(R_i(t)), \quad \chi_4^S(t) = \frac{L}{k_B T} \frac{\langle \mathcal{Q}_S^2 \rangle - \langle \mathcal{Q}_S \rangle^2}{N^2}. \quad (5.9)$$

Since Glotzer *et al.* [13] reported that the contribution of the self part ( $i = j$ ) is dominant over that of the distinct part ( $i \neq j$ ), it is justifiable to calculate  $\chi_4^S$  instead of  $\chi_4$ . Secondly, as the overlap function  $\bar{\delta}_a$ , we adopt a Gaussian function

$$\bar{\delta}_a(r) = e^{-r^2/a^2} \quad (5.10)$$

instead of the step function used by Glotzer *et al.* [13]. We note that, although there exists a variant of  $\chi_4$  from whose definition the probe length can be totally expelled [46], the probe length  $a$  is indispensable to  $\mathcal{Q}_S$ .

From Eq. (4.11) we already know the covariance  $\langle R_i R_j \rangle$  for all  $(i, j)$  and for arbitrary  $t$  (within a certain limitation, of course). The problem is how to evaluate  $\langle \mathcal{Q}_S \rangle$  and  $\langle \mathcal{Q}_S^2 \rangle$  in Eq. (5.9) using this information. This is possible, if we assume that  $(R_1, R_2, \dots, R_N)$  is subject to a joint (multivariate) Gaussian distribution, which is determined uniquely as the covariance is given and the mean is known to vanish. For the purpose of calculating  $\langle \mathcal{Q}_S^2 \rangle$ , it suffices to determine the two-body distribution function for  $(R_i, R_j)$ , which we denote with

$$\begin{aligned} P(R_i, R_j) &= \frac{1}{2\pi\sqrt{\Delta_{ij}}} \exp \left[ -\frac{\langle R^2 \rangle (R_i^2 + R_j^2) - 2 \langle R_i R_j \rangle R_i R_j}{2\Delta_{ij}} \right] \end{aligned}$$

where

$$\Delta_{ij} = \langle R^2 \rangle^2 - \langle R_i R_j \rangle^2, \quad \langle R^2 \rangle = \langle R_i^2 \rangle = \langle R_j^2 \rangle.$$

Using this joint distribution function  $P(R_i, R_j)$  and adopting Eq. (5.10) for the overlapping function, we ob-

tain

$$\begin{aligned}\langle \bar{\delta}_a(R_i) \rangle &= \int \bar{\delta}_a(R_i) P(R_i, R_j) dR_i dR_j \\ &= \frac{1}{\sqrt{1 + \frac{2\langle R^2 \rangle}{a^2}}}\end{aligned}\quad (5.11)$$

and

$$\begin{aligned}\langle \bar{\delta}_a(R_i) \bar{\delta}_a(R_j) \rangle &= \int \bar{\delta}_a(R_i) \bar{\delta}_a(R_j) P(R_i, R_j) dR_i dR_j \\ &= \frac{1}{\sqrt{\left(1 + \frac{2\langle R^2 \rangle}{a^2}\right)^2 - \frac{4\langle R_i R_j \rangle^2}{a^4}}};\end{aligned}\quad (5.12)$$

---


$$\begin{aligned}\chi_4^S &= \frac{L}{N^2 k_B T} \left\{ \sum_i \sum_j \langle \bar{\delta}_a(R_i) \bar{\delta}_a(R_j) \rangle - \left[ \sum_i \langle \bar{\delta}_a(R_i) \rangle \right]^2 \right\} \\ &= \frac{L}{N k_B T} \sum_l \left[ \frac{1}{\sqrt{\left(1 + \frac{2\langle R^2 \rangle}{a^2}\right)^2 - \frac{4\langle R_i R_{i+l} \rangle^2}{a^4}}} - \frac{1}{1 + \frac{2\langle R^2 \rangle}{a^2}} \right].\end{aligned}\quad (5.13)$$


---

Note that the double summation  $\sum_i \sum_j \langle \bar{\delta}_a(R_i) \bar{\delta}_a(R_j) \rangle$  in Eq. (5.13) is a result of the simplification by the replacement of  $\chi_4$  with  $\chi_4^S$  (retaining only the self part): if this simplification were not introduced, we would have to struggle with a quadruple summation such as

$$\sum_i \sum_j \sum_k \sum_l \langle \bar{\delta}_a(X_j(t) - X_i(0)) \bar{\delta}_a(X_l(t) - X_k(0)) \rangle,$$

whose evaluation would be much less workable than  $\langle \bar{\delta}_a(R_i) \bar{\delta}_a(R_j) \rangle$ .

Before applying Eq. (5.13) to SFD, we can test it with free Brownian particles. From the Langevin equation obtained by setting  $V = 0$  in Eq. (1.5), we have

$$\langle R_i R_j \rangle = \begin{cases} \langle R^2 \rangle = 2D [t - \tau_B (1 - e^{-t/\tau_B})] & (i = j) \\ 0 & (i \neq j) \end{cases}\quad (5.14)$$

where  $\tau_B = m/\mu$ . This is substituted into Eq. (5.13), which yields

$$\begin{aligned}\chi_4^S &= \frac{1}{\rho_0 k_B T} \left( \frac{1}{\sqrt{1 + 4\langle R^2 \rangle/a^2}} - \frac{1}{1 + 2\langle R^2 \rangle/a^2} \right) \\ &= (\chi_4^S)_{\text{solo}}\end{aligned}\quad (5.15)$$

note that Eq. (5.12) is confirmed separately for  $i \neq j$  and  $i = j$ . With Eq. (5.11) and (5.12), now we can evaluate  $\chi_4^S$  in Eq. (5.9), taking the uniformity of the system into account. As a result, we obtain

for free Brownian particles; note that all the contribution comes from the term with  $l = 0$  in Eq. (5.13), which we refer to as the “solo” part. Taking notice of the  $t$ -dependence of  $\langle R^2 \rangle$  in Eq. (5.15) and making some calculation, we find  $(\chi_4^S)_{\text{solo}}$  to have a peak at the instant when  $\langle R^2 \rangle = 2.6 a^2$  approximately; see the short-time side of Fig. 7(a). Obviously, this short-time peak is irrelevant to particle interaction. After this peak,  $(\chi_4^S)_{\text{solo}}$  decreases monotonically toward zero, in proportion to  $t^{-1/2}$  for  $t \rightarrow +\infty$ .

Now let us calculate  $\chi_4^S$  for SFD, combining Eq. (5.13) with the result for  $\langle RR \rangle$  in Eq. (4.11). We evaluate  $\chi_4^S$  in Eq. (5.13) as a sum of the “solo” part ( $l = 0$ ) and the collective part (contribution from the terms with  $l \neq 0$ ). The solo part is given by Eq. (5.15) and depends on  $\langle R^2 \rangle$  alone, for which we use Eq. (4.12) that was obtained by setting  $\xi = \xi'$  in Eq. (4.11). As a matter of course, we must exclude cases of very short time, for which Eq. (4.12) predicts  $\langle R^2 \rangle$  to be negative; this is out of the validity range of Eq. (4.12). Subsequently, to evaluate the contribution from the terms with  $l \neq 0$ , we use the asymptotic form of Eq. (4.11) for  $t \rightarrow +\infty$ , expressed

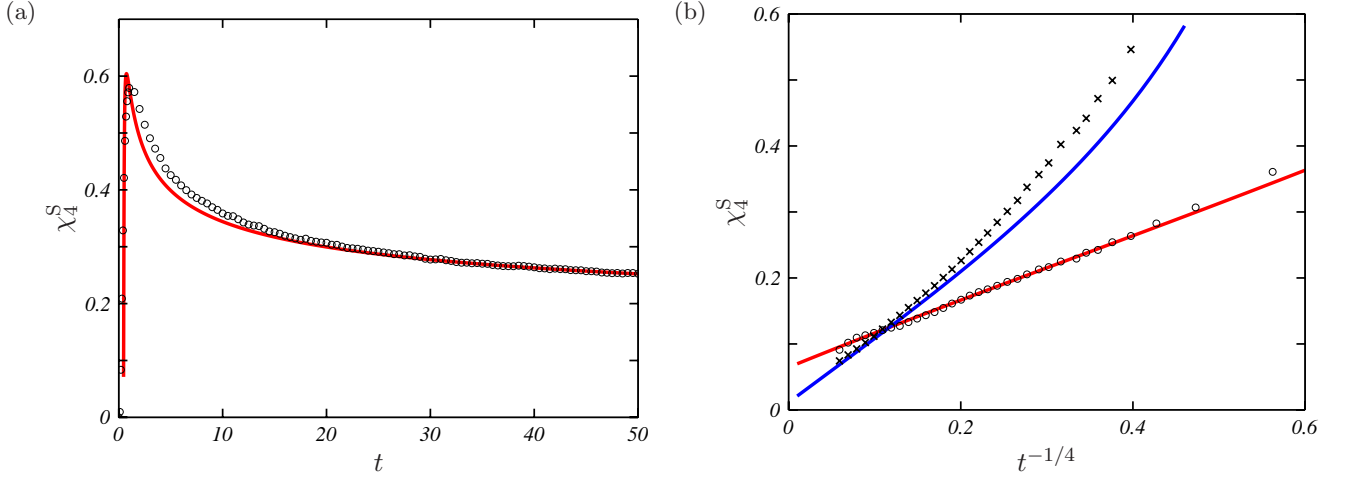


FIG. 7: (Color online) Short-time and longtime behavior of  $\chi_4^S$  for SFD, compared with the analytical prediction given by the sum of  $(\chi_4^S)_{\text{solo}}$  in Eq. (5.15) and  $(\chi_4^S)_{\text{coll}}$  in Eq. (5.17), with the effect of  $S \neq 1$  and  $D_c/D \neq 1$  taken into account. The probe length (radius of the overlapping function) was chosen as  $a = 0.5\sigma$ . The time is non-dimensionalized with  $\sigma^2/D$ . (a) Short-time behavior for the case with  $N = 256$  and  $\rho_0 = N/L = (1/4)\sigma^{-1}$ . The computed data are plotted with circles and the analytical prediction is shown with a solid (red) line. (b) Long-time behavior for  $\rho_0 = (1/4)\sigma^{-1}$  (plotted with circles) and for  $\rho_0 = (1/16)\sigma^{-1}$  (plotted with crosses). The solid lines show analytical prediction for the two cases. Note the asymptotic behavior of the curves that takes the form of a straight line in the graph, exhibiting the decay of  $(\chi_4^S)_{\text{solo}}$  in proportion to  $t^{-1/4}$  and the finite value of  $(\chi_4^S)_{\text{coll}}$  that remains for  $t \rightarrow +\infty$ .

as a self-similar solution in Eq. (3.5):

$$\langle R_i R_{i+l} \rangle \simeq \frac{2\sqrt{Dt}}{\rho_0} \varphi(\theta_l), \quad \theta_l = \frac{l}{\rho_0 \lambda(t)} = l \Delta \theta.$$

The collective part is thereby written as

$$(\chi_4^S)_{\text{coll}} \simeq \frac{1}{\rho_0 k_B T} \times \frac{1}{1 + \frac{2\langle R^2 \rangle}{a^2}} \sum_{l \neq 0} \left\{ \frac{1}{\sqrt{1 - \left[ \frac{\varphi(\theta_l)}{\varphi(0)} \right]^2}} - 1 \right\}.$$

The number of the particle contributing the the sum is estimated to be  $N_{\text{coll}} \sim 1/\Delta \theta = \rho_0 \lambda(t)$ , which yields, approximately,

$$(\chi_4^S)_{\text{coll}} \sim \frac{1}{\rho_0 k_B T} \times \frac{\rho_0 \lambda(t)}{1 + 2\langle R^2 \rangle/a^2} \quad (5.16a)$$

$$\sim \frac{a^2}{k_B T} \times \frac{\lambda(t)}{\langle R^2 \rangle} \sim \frac{a^2 \rho_0}{k_B T} \quad (5.16b)$$

for  $t \rightarrow +\infty$ . More precisely, the sum can be evaluated

by rewriting it as

$$\begin{aligned} \sum_{l \neq 0} (\dots) &= 2\rho_0 \lambda(t) \sum_{l=1}^{\infty} \left\{ \frac{1}{\sqrt{1 - \left[ \frac{\varphi(\theta_l)}{\varphi(0)} \right]^2}} - 1 \right\} \Delta \theta \\ &\rightarrow 2\rho_0 \lambda(t) \int_0^{\infty} \left\{ \frac{1}{\sqrt{1 - \pi [\varphi(\theta)]^2}} - 1 \right\} d\theta \end{aligned}$$

and using the numerical value of the integral

$$\int_0^{\infty} \left\{ \frac{1}{\sqrt{1 - \pi [\varphi(\theta)]^2}} - 1 \right\} d\theta = 0.364124;$$

thus we obtain

$$\begin{aligned} (\chi_4^S)_{\text{coll}} &= \frac{1}{\rho_0 k_B T} \times \frac{\rho_0 \lambda(t)}{\langle R^2 \rangle/a^2} \times 0.364124 \\ &= \frac{1}{\rho_0 k_B T} \times \sqrt{\pi} \rho_0^2 a^2 \times 0.364124 \\ &= 0.6454 \times \frac{\rho_0 a^2}{k_B T} \quad (5.17) \end{aligned}$$

and  $\chi_4^S = (\chi_4^S)_{\text{solo}} + (\chi_4^S)_{\text{coll}}$ , with  $(\chi_4^S)_{\text{solo}}$  given by substituting Eq. (4.12) into Eq. (5.15). If we take  $S$  into account according to Eq. (3.5), the right-hand side of Eq. (5.17) is multiplied by  $S^{-1}$ .

The analytically calculated  $\chi_4^S$  and its numerical values are compared in Fig. 7. The effect of finite  $\rho_0$  that makes

$S$  and  $D_c/D$  different from unity is taken into account (see Table I in Appendix A). The peak in the short-time regime has nothing to do with the slow dynamics, as it appears even for free Brownian particles. After this peak,  $(\chi_4^S)_{\text{solo}}$  decreases slowly, asymptotically in proportion to  $t^{-1/4}$ , while, reflecting the endless growth of the cluster size,  $(\chi_4^S)_{\text{coll}}$  remains finite for  $t \rightarrow +\infty$ . The behavior of the numerical solution is consistent with this analytical prediction.

The limiting value of  $\chi_4^S$  for  $t \rightarrow +\infty$ , given by  $(\chi_4^S)_{\text{coll}}$  in Eq. (5.17), is an increasing function of the density  $\rho_0$ . This conclusion remains unchanged also if the effect of  $S \neq 1$  is included, because  $1/S$  is also an increasing function of  $\rho_0$ .

## VI. DISCUSSION AND CONCLUDING REMARKS

We have studied one-dimensional systems of Brownian particles with repulsive interaction, regarding it as a simplified model of the cage effect. On one hand, the cage confines every particle in a narrow space. On the other hand, since the particles are mutually caged and therefore forbidden to move uncooperatively, they must either wait still or move together. Thus the cage effect involves correlated motion of numerous particles, which is visualized as dynamical clusters in space-time diagrams (Fig. 3), with the diffusive correlation length  $\lambda(t) = 2\sqrt{D_c t}$ . The substance that diffuses is not the particles but the space between them, represented by  $\psi$  in our theory. The two-particle displacement correlation (2pDC) is shown to be a useful indicator of the correlated motion. Asymptotically, 2pDC becomes self-similar: it suggests a matryoshka-like structure, such that the small cages are confined in larger cages, which, in turn, are caught in still larger and slower cages.

Using the analytical result for 2pDC which is valid both transiently and asymptotically, we demonstrated how to calculate the  $Q_S$ -based  $\chi_4$  (denoted with  $\chi_4^S$ ). Despite the endless growth of  $\lambda(t)$  and the absence of  $\alpha$  relaxation, the result in Eq. (5.17) shows that  $\chi_4^S$  converges to some constant for  $t \rightarrow +\infty$ . An implication of Eq. (5.17) is that  $\chi_4^S$ , and probably  $\chi_4$  in general, does not give a straightforward representation of the cluster size. Indeed,  $\lambda(t)$  is in the numerator of Eq. (5.16) or (5.17), but the result is modified by the denominator, or a prefactor  $1/(1 + 2\langle R^2 \rangle/a^2)$  originating from  $\langle Q_S \rangle^2$ , which cancels the temporal growth of the cluster size. In three-dimensional systems, a direct relation between  $\chi_4^S$  and the cluster size is expected only for some limited time scales corresponding to the plateau of the MSD.

The adoption of the Lagrangian description enabled us to reproduce Kollmann's asymptotic law for MSD within the liquid-theoretical framework, calculate 2pDC analytically, and develop the "Lagrangian MCT" without violating FDT. The Lagrangian MCT equation was solved approximately by analytical means, giving a finite-time

correction to the asymptotic law. We have implemented the Lagrangian description by explicitly introducing the label variable  $\xi$  and thereby constructing a stretchable coordinate system that sticks to the cages everywhere. Probably some aspects of glassy dynamics, such as dynamical heterogeneity characterizable by bond breaking [3, 63, 65], may require the Lagrangian description by nature when its continuum counterpart is sought.

The Lagrangian description in higher dimensions may not be so simple as in one-dimensional cases, but it is not impossible. In three-dimensional cases, a triplet of label variables  $(\xi, \eta, \zeta)$  is expected to be related with  $\rho$  and  $\mathbf{Q}$  by equations analogous to Eq. (2.5); see Eqs. (6.6) and (6.7) in Ref. [24]. Besides, we could adopt some methods from three-dimensional theories of turbulence in which Lagrangian correlations are used [30–32]. Turbulence theoreticians have even considered the Lagrangian dynamics of a tetrad (four material points) [66], whose two-time correlation involves eight points in the space-time.

In contrast to the "Eulerian" (standard) MCT in which cage effects are represented by the memory kernel (not successful in SFD), the Lagrangian theory can dispense with the memory integral as far as the asymptotic behavior is concerned. A pivotal role is played by the modified and extended Alexander–Pincus formulae in Eqs. (2.15) and (3.2). Its linear version, namely Eq. (2.17) or its multidimensional extension, has been used in the context of glassy dynamics by several authors [5, 43], who limited themselves to the approximation with linear elasticity. Since the Eulerian and the Lagrangian variables are approximately interchangeable in the description of small elastic deformation, they did not bother to distinguish the two descriptions. Needless to say, this treatment fails when the system is more liquid-like. In an attempt to introduce the  $\alpha$  relaxation into the calculation of  $\chi_4$  based on the "elastic" theory, Toninelli *et al.* feared that it would make the model inconsistent, because the underlying lattice, needed to define the deformation field, would be totally melted [5]. Probably this is too pessimistic: the "melting" of the lattice does not make the theory totally inconsistent but requires more careful distinction between the Eulerian and the Lagrangian coordinates.

There will be another modification to the theory of Toninelli *et al.*, when departing from the linear elasticity and trying to consider liquid-like behavior. Their formula corresponding to Eq. (3.2), namely Eq. (A3) in Ref. [5], reads

$$\langle R(\tilde{\mathbf{d}})R(\mathbf{0}) \rangle \propto \int \frac{1 - e^{-D\mathbf{k}^2 t}}{\mathbf{k}^2} e^{-i\mathbf{k} \cdot \tilde{\mathbf{d}}} d^n \mathbf{k} \quad (6.1)$$

in our notation, as they seem to have identified the Langevin equation for the displacement field with the Edwards–Wilkinson equation [42]. In regard to Eq. (6.1), we suspect that the vectorial character of the displacement is not adequately taken into account. Probably one needs to decompose  $\mathbf{R}$  into the longitudinal and transverse components, and tract them more carefully. Unlike



the two sound modes in elastic solids, the two modes in the liquids can have quite different nature: the liquid may resist compression strongly but the resistance to shear may be much weaker.

In Eq. (5.6), we have proposed to define the three-dimensional 2pDC as a tensorial quantity  $\mathbf{X}$ . Due to the isotropy of the system,  $\mathbf{X}$  must be a sum of the longitudinal and the transverse components:

$$\mathbf{X} = X_{\parallel} \frac{\tilde{\mathbf{d}} \otimes \tilde{\mathbf{d}}}{\tilde{d}^2} + X_{\perp} \left( \mathbb{1} - \frac{\tilde{\mathbf{d}} \otimes \tilde{\mathbf{d}}}{\tilde{d}^2} \right).$$

It is quite likely that  $X_{\parallel}$  and  $X_{\perp}$  will be characterized by different correlation lengths. Taking the two different correlation lengths into account, we can extend the present theory phenomenologically to the three-dimensional cases. From the inferred distribution function for the displacements of two particles, shown in Appendix C, we can calculate  $\chi_4^S$  in the same way as in Subsec. VB, as

$$\chi_4^S \sim \frac{1}{k_B T} \times \frac{(1 - \alpha)^2 \lambda_{\parallel} \lambda_{\perp}^2}{\left(1 + \frac{2X^0}{a^2}\right)^3}, \quad (6.2)$$

where  $\lambda_{\parallel} = \lambda_{\parallel}(t)$  and  $\lambda_{\perp} = \lambda_{\perp}(t)$  denote the two correlation lengths,  $X^0 = X^0(t)$  is related to the MSD of the caged particles, and  $\alpha = \alpha(t)$  stands for the relative number of the particles that have hopped. Assuming the  $t$ -dependence of these four quantities phenomenologically as

$$\lambda_{\parallel} = \frac{\sqrt{Dt}}{1 + \sqrt{t/\tau}}, \quad \lambda_{\perp} = \left(1 + \sqrt{t/\tau}\right) \ell_0, \\ X_0 = \frac{Dt}{1 + Dt/\ell_0^2}, \quad \alpha = \tanh \frac{t}{\tau},$$

we can plot  $\chi_4^S$  against  $t$  for some different values of the time scale  $\tau$ . The curves in Fig. 8 reproduce some basic features of the  $\mathcal{Q}$ -based  $\chi_4$  calculated by Lačević *et al.* [14], such as the shape of the uphill that looks steeper near the peak in this semi-log plot.

To go beyond the linear theory,  $n_d$ -dimensional versions of the extended Alexander–Pincus formula should be developed. We suppose that the  $n_d$ -dimensional formula will contain, instead of  $\tilde{C}$ , correlations of *deformation tensor*. This is not so formidable as it may appear, because many components of the correlation tensor will turn out to vanish or to have the same value as some other component. The formula is now under development and will be reported elsewhere.

It is also noteworthy that, in the derivation of MCT, the difficulty of FDT violation disappeared quite naturally due to the Lagrangian description. As is pointed out by Miyazaki & Reichman [39], it has been difficult to construct realistic models which does not violate FDT and can incorporate the effect of structural changes embodied in  $S(k)$  at the same time. Since the “Lagrangian

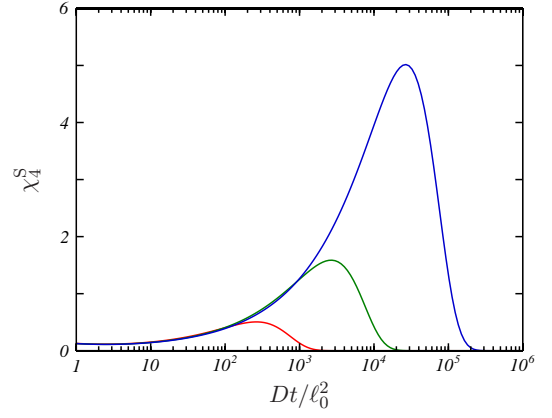


FIG. 8: (Color online) Behavior of  $\chi_4^S$  given by Eq. (6.2), calculated through the three-dimensional two-body displacement distribution function by phenomenologically extending the present theory to the three-dimensional cases. The three curves correspond to different values of  $\tau$ : from left to right,  $\tau = 10^3 \ell_0^2/D$ ,  $10^4 \ell_0^2/D$ , and  $10^5 \ell_0^2/D$ .

MCT” is now shown to be consistent with FDT, study of its behavior for different  $S(k)$  may be quite intriguing.

For possible extensions in the future, we can mention several directions. For example, one may include weak attractive interaction and analyze the effect of the change in  $S(k)$  on the transient behavior of SFD. One may also study nonequilibrium behavior by driving the particles with an external force or changing the temperature suddenly. Another interesting proposal is to permit overtaking as a rare event, which may play the role of the  $\alpha$  relaxation. We performed simulations with some finite interaction potential, and a preliminary result [67] shows that normal diffusion is observed for  $V_{\max} = k_B T$ , while for  $V_{\max} = 5k_B T$  the behavior is essentially that of SFD in the time scale of the simulation. The problem is to make a theory that can handle the crossover between the two limiting cases. The theory allowing for rare overtaking events may bridge the gap between the purely one-dimensional SFD and the behavior of three-dimensional rod polymers [16, 68].

We could also study *double-file diffusion*, which would be analogous to two-lane models of traffic flows. If a “lane interaction” is also introduced, the system would have also something common with the Matsukawa–Fukuyama model of friction formulated on a ladder lattice [69, 70]. The study of the double-file diffusion may shed light to many related systems in which frustration is dynamically created and annihilated, such as template-assisted pattern formation of colloid particles on a substrate with parallel channels [71], frustrated Josephson-junction arrays in a magnetic field [70, 72], and—hopefully—also three-dimensional dense colloidal suspensions.

The present work, in combination with the previous one [24], is intended as several first steps toward a future theory of three-dimensional glassy liquids, which will make it possible, for example, to replace the semi-

phenomenological curves for  $\chi_4^S$  in Fig. 8 with a first-principle theoretical calculation. Although the present theory is still embryonic, it already suggests that one of the important ingredients of the future theory may be the displacement distribution function of two or more particles. In the case of computational analysis, probably we should not insist on some favorite statistical quantity alone, nor content ourselves with the single-particle van Hove function, but try to deduce some suitable distribution function behind the computed statistical quantities. The present analysis of one-dimensional cage dynamics and the concepts used for it will provide a useful framework both for analysis of numerical data and for new development of theory of glassy liquids.

### Acknowledgments

We express our cordial gratitude to Kunimasa Miyazaki, Shin-ichi Sasa, Takeshi Kawasaki, and So Kitsunezaki for valuable comments and fruitful discussions. This work was supported by Grants-in-Aid for Scientific Research (KAKENHI) (C) No. 21540388 and (C) No. 24540404, JSPS (Japan).

### Appendix A: Numerical calculations

Here we describe how we integrated the one-dimensional Langevin equation (1.5), and also how we evaluated the statistical quantities, including  $\langle R^2 \rangle$ ,  $D_c$ , and  $S$ , from the numerical solution. As the system contains  $N$  particles in a periodic box of the size  $L$ , the mean density is given by  $\rho_0 = N/L$ .

The potential  $V$  in Eq. (1.5) was specified as

$$V(r) = \begin{cases} V_{\max} \left(1 - \frac{|r|}{\sigma}\right)^2 & (|r| \leq \sigma) \\ 0 & (|r| > \sigma) \end{cases} \quad (\text{A1})$$

with  $V_{\max} \gg k_B T$ . In the present numerical calculations we adopted the value  $V_{\max} = 50 k_B T$ , which is high enough to forbid the overtaking of the particles completely.

The random forcing is the zero-mean Gaussian noise whose variance is given by the one-dimensional version of Eq. (1.2),

$$\langle f_i(t) f_j(t') \rangle = 2D \delta_{ij} \delta(t - t'). \quad (\text{A2})$$

Computationally, the delta function in Eq. (A2) was discretized with the time interval  $\Delta t_f$ , and as the values of  $(f_0, f_1, \dots, f_{N-1})$  for each time interval,  $N$  independent Gaussian random numbers with the variance  $2D/\Delta t_f$  were generated with the Mersenne twister and the Box-Muller transform.

With  $V$  and  $f_i$  given as above, in nondimensionalization of the governing equation using  $\sigma$ ,  $\sigma^2/D$ , and  $m$

as the units of length, time, and mass, there appears a nondimensional parameter specifiable as the ratio of  $\tau_B = m/\mu$  to the time unit  $\sigma^2/D$ , which we chose as 1 : 1. Then the time integration of Eq. (1.5) was performed with a Verlet-like scheme. The time step  $\Delta t$  was taken equal to a hundredth of the time unit  $\sigma^2/D$ , and the renewal interval of the random forcing,  $\Delta t_f$ , was chosen to be the same as the time step:

$$\Delta t = \Delta t_f = 10^{-2} \times \frac{\sigma^2}{D}. \quad (\text{A3})$$

We also tested some different choices of  $\Delta t$  and  $\Delta t_f$ , such as

$$\frac{(\Delta t, \Delta t_f)}{\sigma^2/D} = (10^{-3}, 10^{-3}) \quad \text{or} \quad (10^{-3}, 10^{-2}).$$

To bring the system into equilibrium, we started each calculation at  $t = -\mathcal{T}_w$ , introducing a sufficiently long waiting time  $\mathcal{T}_w$  (typically  $\mathcal{T}_w = 10^4 \sigma^2/D$ ), and waited till  $t = 0$ . Then, from the simulation data recorded for  $0 \leq t \leq t_{\max}$ , we calculated a desired statistical quantity as the average for  $n$  samples extracted from the data by a time shift. For example,  $\langle R^2 \rangle$  is calculated as

$$\langle R(t')^2 \rangle = \frac{1}{nN} \sum_{l=0}^{n-1} \sum_{i=0}^{N-1} [X_i(t_l + t') - X_i(t_l)]^2, \quad (\text{A4})$$

where  $t_l$  denotes the starting time of the  $l$ -th sample. Care must be taken so that the maximal value of  $t'$  in Eq. (A4), which equals the span of each sample, should not exceed the waiting time  $\mathcal{T}_w$ ; a result for a longer span will expose insufficiency of equilibration. Typically we chose  $t_{\max} = 5\mathcal{T}_w$ ,  $n = 100$ , and  $t_l = l(t_{\max} - \mathcal{T}_w)/n$ , allowing the samples to overlap.

The computation of  $X_R(\tilde{d}, t)$ , shown in Fig. 6, was performed with discretization of Eq. (5.2) in which the delta function was approximated by a statistical bin  $0.5\sigma$  in width. After recording  $X_i(t_l)$  for every particle, we classified every pair  $(i, j)$  into a statistical bin according to the “initial” distance  $X_j(t_l) - X_i(t_l)$ , so that the  $\kappa$ -th bin contains the pairs for which  $|X_j(t_l) - X_i(t_l) - \tilde{d}_\kappa|$  is smaller than the half width of the bin. Then we calculated  $X_R(\tilde{d}_\kappa, t)$  as the average of  $R_i(t)R_j(t)$  for the  $\kappa$ -th bin, where  $R_i(t) = X_i(t_l + t) - X_i(t_l)$ . If, instead, the sum of the absolute values of the data in each bin were calculated, this would be analogous to the quantity studied by Donati *et al.* [37].

The collective diffusion coefficient  $D_c$  is determined from the temporal decay of the dynamical structure factor  $F(q, t)$  [26]. We computed  $F(q, t)$  for  $0 < q \ll \rho_0$  and made a linear fit for  $\log F(q, t) = \log S(q) - D_c q^2 t$  to obtain the values of  $S(q)$  and  $D_c$  as the fitting parameters. After taking an average for several small values of  $q$ , the results are summarized in Table I. These values are used in evaluation of the theoretical predictions, such as Eq. (3.3), and also for rescaling of the horizontal axis in Fig. 5.

TABLE I: Numerical values of  $S(0)$  and  $D_c/D$  computed for three different values of the density.

| $\rho_0$            | $(1/4)\sigma^{-1}$ | $(1/8)\sigma^{-1}$ | $(1/16)\sigma^{-1}$ |
|---------------------|--------------------|--------------------|---------------------|
| $1 - 2\rho_0\sigma$ | 0.500              | 0.750              | 0.875               |
| $S(0)$              | 0.624              | 0.787              | 0.888               |
| $D_c/D$             | 1.59               | 1.27               | 1.12                |
| $S(0)\sqrt{D_c/D}$  | 0.79               | 0.89               | 0.94                |

## Appendix B: Direct-interaction approximation

The main idea of DIA [29, 53] for evaluation of the triple correlation

$$\langle \check{\psi}(-p, t) \check{\psi}(-q, t) \check{\psi}(-k, 0) \rangle = \langle \check{\psi}(p, t) \check{\psi}(q, t) \check{\psi}(k, 0) \rangle^*,$$

with the asterisk denoting the complex conjugate, is to utilize the property of  $\mathcal{V} = (\mathcal{V}_\alpha^{\beta\gamma})$  that, out of its  $N^3$  components, almost all are zero because the condition  $\alpha + \beta + \gamma = 0$  is not satisfied. The nonzero components of  $\mathcal{V}$  constitute what we call triad interactions: rewriting Eq. (2.12) as

$$(\partial_t + \mu_\alpha) \check{\psi}(\alpha, t) = \sum \mathcal{V}_\alpha^{\beta\gamma} \check{\psi}^*(\beta, t) \check{\psi}^*(\gamma, t) + \rho_0 \check{f}_L(\alpha, t) \quad (2.12')$$

makes it clearer that  $\mathcal{V}_\alpha^{\beta\gamma}$  engages in connecting the “triad” that consists of  $\alpha$ ,  $\beta$ , and  $\gamma$ . If we visualize each triad interaction as a triangle on a graph, the property of  $\mathcal{V}$  is such that no triangle shares its side with other triangles. Therefore, if we “switch off” a single triad, say,  $\{p, q, k\}$  (with which we mean  $\mathcal{V}_k^{pq}$ ,  $\mathcal{V}_k^{qp}$ ,  $\mathcal{V}_p^{qk}$ ,  $\mathcal{V}_p^{kq}$ ,  $\mathcal{V}_q^{kp}$ , and  $\mathcal{V}_q^{pk}$ ; note the symmetry in regard to the interchange of the superscripts,  $\mathcal{V}_k^{pq} = \mathcal{V}_k^{qp}$  etc.), the *direct interactions* between the three modes  $p, q, k$  are lost.

To concretize this idea, let us suppose that an artificial forcing term

$$I_\alpha = -\theta(t-t_0) \frac{N}{L^2} \times \begin{cases} 2\mathcal{V}_k^{pq} \check{\psi}^*(p, t) \check{\psi}^*(q, t) & (\alpha = k) \\ 2\mathcal{V}_p^{qk} \check{\psi}^*(q, t) \check{\psi}^*(k, t) & (\alpha = p) \\ 2\mathcal{V}_q^{kp} \check{\psi}^*(k, t) \check{\psi}^*(p, t) & (\alpha = q) \\ 0 & (\text{otherwise}), \end{cases}$$

designed to cancel a single triad  $\{p, q, k\}$ , is applied to the system given by Eq. (2.12'). We denote the solution to this artificial system with  $\check{\psi}_0 = \check{\psi}_0(\{p, q, k\}; \alpha, t)$ . One of the two main assumptions of DIA is that the three selected modes, namely  $\check{\psi}_0(p, t)$ ,  $\check{\psi}_0(q, t)$ , and  $\check{\psi}_0(k, t)$  in this case, become uncorrelated, since the forcing  $I$  cancels the direct interactions. On the other hand,  $I$  is regarded as a small perturbation, because it cancels only a single triad interaction and there remain still a large number of triads connecting, say,  $p$  and  $q$  indirectly. Therefore the difference  $\check{\psi}_1 = \check{\psi} - \check{\psi}_0$  is assumed to be small, which is the second main assumption of DIA.

Due to these assumptions, the triple correlation is ex-

panded as

$$\begin{aligned} \langle \check{\psi}(p, t) \check{\psi}(q, t) \check{\psi}(k, 0) \rangle &= \langle \check{\psi}_0(p, t) \check{\psi}_0(q, t) \check{\psi}_0(k, 0) \rangle \\ &+ \langle \check{\psi}_1(p, t) \check{\psi}_0(q, t) \check{\psi}_0(k, 0) \rangle \\ &+ \langle \check{\psi}_0(p, t) \check{\psi}_1(q, t) \check{\psi}_0(k, 0) \rangle \\ &+ \langle \check{\psi}_0(p, t) \check{\psi}_0(q, t) \check{\psi}_1(k, 0) \rangle \\ &+ O(\check{\psi}_1^2), \end{aligned} \quad (B1)$$

and the zero-th term,  $\langle \check{\psi}_0(p, t) \check{\psi}_0(q, t) \check{\psi}_0(k, 0) \rangle$ , vanishes. Since  $I$  is a small perturbation and  $\check{\psi}_1$  is a response to it, formally  $\check{\psi}_1$  can be expressed in terms of the propagator  $G$  as

$$\check{\psi}_1(\alpha, t) = - \int_{t_0}^t dt' \sum_{\alpha'} G(\alpha, t; \alpha', t') I_{\alpha'}(t') \quad (B2)$$

for  $t > t_0$ . We substitute Eq. (B2) into each term on the right-hand side of Eq. (B1) to find, to our surprise, that the result is *naturally factorized* due to the assumption of DIA that  $\check{\psi}_0(p, t)$ ,  $\check{\psi}_0(q, t)$ , and  $\check{\psi}_0(k, t)$  are uncorrelated.

By applying the decomposition  $\check{\psi} = \check{\psi}_0 + \check{\psi}_1$  to each triple correlation term in the equation for  $\partial_t \check{C}$ , we are led to Eq. (4.1). Similarly, the equation for  $\partial_t \check{G}$  contains  $\langle \check{\psi}_0 G \rangle$ , which is evaluated with the aid of the DIA decomposition of  $G$ , resulting in Eq. (4.2). For more details, see Refs. [53, 54].

## Appendix C: Three-dimensional calculation of $\chi_4^S$

Here we outline how to calculate  $\chi_4^S$  by phenomenologically extending the present theory to the three-dimensional cases. The displacement correlation tensor  $\mathbf{X}$  is related to the distribution function  $P(\tilde{\mathbf{d}}; \mathbf{R}_i, \mathbf{R}_j)$  by

$$\mathbf{X}(\tilde{\mathbf{d}}) = \iint \mathbf{R}_i \otimes \mathbf{R}_j P(\tilde{\mathbf{d}}; \mathbf{R}_i, \mathbf{R}_j) d^3 \mathbf{R}_i d^3 \mathbf{R}_j;$$

in what follows, the  $\tilde{\mathbf{d}}$ -dependence of  $P$  is taken for granted and therefore omitted. The relation can be inverted if the functional form of  $P$  is known. In particular, if a multivariate Gaussian distribution (which we denote with  $P_0$ ) is assumed,  $P = P_0$  can be factorized as

$$P_0(\mathbf{R}_i, \mathbf{R}_j) = P_{\parallel}(\mathbf{R}_i^{\parallel}, \mathbf{R}_j^{\parallel}) P_{\perp}(\mathbf{R}_i^{\perp}, \mathbf{R}_j^{\perp}) \quad (C1)$$

by splitting  $\mathbf{R}$  into the longitudinal and transverse components as  $\mathbf{R} = \mathbf{R}^{\parallel} + \mathbf{R}^{\perp}$  (so that  $\mathbf{R}^{\parallel} \parallel \tilde{\mathbf{d}}$  and  $\mathbf{R}^{\perp} \perp \tilde{\mathbf{d}}$ ). Then we introduce  $X^0$  such that

$$X_{\parallel}(\tilde{\mathbf{d}} = 0) = X_{\perp}(\tilde{\mathbf{d}} = 0) = X^0$$

and write the two factors explicitly as

$$P_{\parallel} = \frac{1}{2\pi\sqrt{\Delta_{\parallel}}} \exp \left[ -\frac{X^0(R_i^{\parallel 2} + R_j^{\parallel 2}) - 2X_{\parallel}(\tilde{d})R_i^{\parallel}R_j^{\parallel}}{2\Delta_{\parallel}} \right],$$

$$P_{\perp} = \frac{1}{(2\pi)^2\Delta_{\perp}} \times \exp \left[ -\frac{X^0(\mathbf{R}_i^{\perp 2} + \mathbf{R}_j^{\perp 2}) - 2X_{\perp}(\tilde{d})\mathbf{R}_i^{\perp} \cdot \mathbf{R}_j^{\perp}}{2\Delta_{\perp}} \right],$$

where  $\Delta_{\parallel} = (X^0)^2 - X_{\parallel}(\tilde{d})^2$  etc.

Then the calculation of  $\chi_4^S$  will be carried out in a way analogous to the 1D cases. Subsequently, assuming that two correlation lengths,  $\lambda_{\parallel} = \lambda_{\parallel}(t)$  and  $\lambda_{\perp} = \lambda_{\perp}(t)$ , can be introduced so that

$$X_{\parallel} \sim X^0(t) \Phi_{\parallel}(\tilde{d}/\lambda_{\parallel}(t)),$$

$$X_{\perp} \sim X^0(t) \Phi_{\perp}(\tilde{d}/\lambda_{\perp}(t)),$$

we estimate the number of the particles contributing to the sum as  $N_{\text{coll}} \sim \rho_0 \lambda_{\parallel} \lambda_{\perp}^2$ , which leads to

$$\chi_4^S \sim \frac{1}{k_B T} \times \frac{\lambda_{\parallel} \lambda_{\perp}^2}{\left(1 + \frac{2X^0}{a^2}\right)^3} \quad (\text{C2})$$

as a three-dimensional counterpart of Eq. (5.16a).

Of course, Eq. (C2) needs to be modified by taking  $\alpha$  relaxation into account. We introduce  $\alpha = \alpha(t)$  denoting

the relative number of the particles that have hopped by the time  $t$ , and assume the distribution function in the form

$$P(\mathbf{R}_i, \mathbf{R}_j) = \begin{cases} (1 - \alpha)^2 P_0 + 2\alpha(1 - \alpha)P_1 + \alpha^2 P_2 & (i \neq j) \\ (1 - \alpha)P_0 + \alpha P_2 & (i = j), \end{cases} \quad (\text{C3})$$

where  $P_0$ , governing the pairs of caged particles, is given by Eq. (C1). Note that, by integrating  $P(\mathbf{R}_i, \mathbf{R}_j)$  in regard to the second argument  $\mathbf{R}_j$ , Eq. (C3) reduces to the van Hove function in the form

$$P(\mathbf{R}) = (1 - \alpha)P_{\text{cage}}(\mathbf{R}) + \alpha P_{\text{hop}}(\mathbf{R}).$$

This implies that  $\alpha = \alpha(t)$  can be determined, in principle, as a fitting parameter for the van Hove function. If we assume, for simplicity, that the correlation of displacements is totally lost after the hopping, we have

$$P_1(\mathbf{R}_i, \mathbf{R}_j) = \frac{P_{\text{hop}}(\mathbf{R}_i)P_{\text{cage}}(\mathbf{R}_j) + P_{\text{cage}}(\mathbf{R}_i)P_{\text{hop}}(\mathbf{R}_j)}{2},$$

$$P_2(\mathbf{R}_i, \mathbf{R}_j) = P_{\text{hop}}(\mathbf{R}_i)P_{\text{hop}}(\mathbf{R}_j).$$

Using the distribution function in Eq. (C3) supplemented with the above expressions, we evaluate  $\chi_4^S$  and obtain Eq. (6.2).

- 
- [1] A. J. Liu and S. R. Nagel, *Jamming and Rheology: Constrained Dynamics on Microscopic and Macroscopic Scales* (Taylor & Francis, London, 2001).
  - [2] L. Berthier and G. Biroli, Rev. Mod. Phys. **83**, 587 (2011).
  - [3] R. Yamamoto and A. Onuki, Phys. Rev. E **58**, 3515 (1998).
  - [4] L. Berthier, G. Biroli, J.-P. Bouchaud, L. Cipelletti, and W. van Saarloos, eds., *Dynamical Heterogeneities in Glasses, Colloids, and Granular Media* (Oxford University Press, Oxford, 2011).
  - [5] C. Toninelli, M. Wyart, L. Berthier, G. Biroli, and J.-P. Bouchaud, Phys. Rev. E **71**, 041505 (2005).
  - [6] G. Biroli, J.-P. Bouchaud, K. Miyazaki, and D. R. Reichman, Phys. Rev. Lett. **97**, 195701 (2006).
  - [7] W. Götze and L. Sjögren, Rep. Prog. Phys. **55**, 241 (1992).
  - [8] D. R. Reichman and P. Charbonneau, J. Stat. Mech. p. P05013 (2005).
  - [9] K. Miyazaki, Bussei Kenkyū **88**, 621 (2007), [in Japanese].
  - [10] D. Hilbert, Göttinger Nachrichten pp. 253–297 (1900), in German.
  - [11] W. Kob and H. C. Andersen, Phys. Rev. Lett. **73**, 1376 (1994).
  - [12] B. Doliwa and A. Heuer, Phys. Rev. E **61**, 6898 (2000).
  - [13] S. C. Glotzer, V. N. Novikov, and T. B. Schröder, J. Chem. Phys. **112**, 509 (2000).
  - [14] N. Lačević, F. W. Starr, T. B. Schröder, and S. C. Glotzer, J. Chem. Phys. **119**, 7372 (2003).
  - [15] C. Donati, S. Franz, S. C. Glotzer, and G. Parisi, J. Non-Cryst. Solids **307-310**, 215 (2002).
  - [16] K. Miyazaki and A. Yethiraj, J. Chem. Phys. **117**, 10448 (2002).
  - [17] T. E. Harris, J. Appl. Probab. **2**, 323 (1965).
  - [18] D. W. Jepsen, J. Math. Phys. **6**, 405 (1965).
  - [19] S. Alexander and P. Pincus, Phys. Rev. B **18**, 2011 (1978).
  - [20] M. Kollmann, Phys. Rev. Lett. **90**, 180602 (2003).
  - [21] A. Taloni and F. Marchesoni, Phys. Rev. Lett. **96**, 020601 (2006).
  - [22] E. Barkai and E. Silbey, Phys. Rev. Lett. **102**, 050602 (2009).
  - [23] E. Barkai and E. Silbey, Phys. Rev. E **81**, 041129 (2010).
  - [24] Ooshida Takeshi, S. Goto, T. Matsumoto, A. Nakahara, and M. Otsuki, J. Phys. Soc. Japan **80**, 074007 (2011).
  - [25] J.-B. Delfau, C. Coste, and M. S. Jean, Phys. Rev. E **85**, 061111 (2012).
  - [26] C. Lutz, M. Kollmann, and C. Bechinger, Phys. Rev. Lett. **93**, 026001 (2004).



- [27] The problem would reduce to that of elastic solids if  $V$  were replaced with a Hookian spring [5, 12, 73], but this is not the case here.
- [28] K. Miyazaki, in *Meeting Abstracts of the Physical Society of Japan (2008 Annual Meeting) Part 2* (2008), p. 393, 26pWE-11 [in Japanese].
- [29] R. H. Kraichnan, *J. Fluid Mech.* **5**, 497 (1959).
- [30] R. H. Kraichnan, *Physics of Fluids* **8**, 575 (1965).
- [31] Y. Kaneda, *J. Fluid Mech.* **107**, 131 (1981).
- [32] S. Kida and S. Goto, *J. Fluid Mech.* **345**, 307 (1997).
- [33] L. D. Landau and E. M. Lifshitz, *Fluid Mechanics*, vol. 6 of *Theoretical Physics* (Butterworth-Heinemann, Oxford, 1987).
- [34] A. Bennett, *Lagrangian fluid dynamics* (Cambridge University Press, Cambridge, 2006), ISBN 0-521-85310-9.
- [35] T. Muranaka and Y. Hiwatari, *Phys. Rev. E* **51**, R2735 (1995).
- [36] Y. Hiwatari and T. Muranaka, *J. Non-Cryst. Solids* **235-237**, 19 (1998).
- [37] C. Donati, S. C. Glotzer, and P. H. Poole, *Phys. Rev. Lett.* **82**, 5064 (1999).
- [38] D. S. Dean, *J. Phys. A: Math. Gen.* **29**, L613 (1996).
- [39] K. Miyazaki and D. R. Reichman, *J. Phys. A: Math. Gen.* **38**, L343 (2005).
- [40] M. Spivak, *Calculus on Manifolds: A Modern Approach to Classical Theorems of Advanced Calculus* (W.A. Benjamin Inc., New York, 1965), ISBN 0-8053-9021-9.
- [41] Terms containing  $\delta_{k,k'\pm N}, \delta_{k,k'\pm 2N}, \dots$  are omitted from Eq. (2.14), as they are not important for the behavior of the long-wave modes.
- [42] S. F. Edwards and D. R. Wilkinson, *Proc. R. Soc. London, Ser. A* **381**, 17 (1982).
- [43] A. Lefèvre, L. Berthier, and R. Stinchcombe, *Phys. Rev. E* **72**, 010301(R) (2005).
- [44] The factor  $L^{-2}$  is included in the definition of  $\tilde{C}$  so that  $\tilde{C}$  has the dimension of the square of the density. It is a matter of choice whether to include it or not.
- [45] K. Honda, *Phys. Rev. E* **55**, R1235 (1996).
- [46] A. Ikeda, L. Berthier, and G. Biroli, arXiv:1209.2814.
- [47] S. P. Das and G. F. Mazenko, *Phys. Rev. A* **34** (1986).
- [48] R. Schmitz, J. W. Dufty, and P. De, *Phys. Rev. Lett.* **71**, 2066 (1993).
- [49] P. C. Martin, E. D. Siggia, and H. A. Rose, *Phys. Rev. A* **8**, 423 (1973).
- [50] B. Kim and K. Kawasaki, *J. Stat. Mech.* p. P02004 (2008).
- [51] T. H. Nishino and H. Hayakawa, *Phys. Rev. E* **78**, 061502 (2008).
- [52] Andreanov, Biroli, and Lefèvre, *J. Stat. Mech.* p. P07008 (2006).
- [53] S. Goto and S. Kida, *Physica D* **117**, 191 (1998).
- [54] Ooshida Takeshi, S. Goto, T. Matsumoto, A. Nakahara, and M. Otsuki, *Progress of Theoretical Physics Supplement* **195**, 157 (2012).
- [55] U. M. B. Marconi, A. Puglisi, L. Rondoni, and A. Vulpiani, *Physics Reports* **461**, 111 (2008).
- [56] H. Risken, *The Fokker-Planck equation: methods of solution and applications* (Springer, 1996), 2nd ed.
- [57] N. G. van Kampen, *Stochastic processes in physics and chemistry* (Elsevier, 2007), 3rd ed.
- [58] In the case of Navier–Stokes turbulence, the self-interaction is assured to vanish due to the incompressibility condition.
- [59] L. Berthier, *Phys. Rev. E* **69**, 020201(R) (2004).
- [60] C. Dasgupta, A. V. Indrani, S. Ramaswamy, and M. K. Phani, *Europhys. Lett.* **15**, 307 (1991).
- [61] O. Dauchot, G. Marty, and G. Biroli, *Phys. Rev. Lett.* **95**, 265701 (2005).
- [62] F. Lechenault, O. Dauchot, G. Biroli, and J. P. Bouchaud, *Europhys. Lett.* **83**, 46002 (2008).
- [63] H. Shiba, T. Kawasaki, and A. Onuki, arXiv:1205.6090.
- [64] Though it may be more appropriate to denote the  $Q_S$ -based  $\chi_4$  with  $\chi_4^{Q_S}$  following the notation of Dauchot *et al.* [61], here we have chosen to write  $\chi_4^S$ . This is actually a somewhat arbitrary choice, which we made simply because it is more friendly to the eyes.
- [65] T. Kawasaki and A. Onuki, arXiv:1210.0369v2.
- [66] M. Chertkov, A. Pumir, and B. I. Shraiman, *Physics of Fluids* **11**, 2394 (1999).
- [67] Ooshida Takeshi, M. Otsuki, S. Goto, A. Nakahara, and T. Matsumoto, *Nagare* **31** (2012), [in Japanese].
- [68] J. M. Rallison, *J. Fluid Mech.* **186**, 471 (1988).
- [69] H. Matsukawa and H. Fukuyama, *Phys. Rev. B* **49**, 17286 (1994).
- [70] H. Yoshino, T. Nogawa, and B. Kim, *Progress of Theoretical Physics Supplement* **184**, 153 (2010).
- [71] C. Mondal and S. Sengupta, *Phys. Rev. E* **85**, 020402(R) (2012).
- [72] H. Yoshino, T. Nogawa, and B. Kim, *Phys. Rev. Lett.* **105**, 257004 (2010).
- [73] J.-B. Delfau, C. Coste, and M. S. Jean, *Phys. Rev. E* **84**, 011101 (2011).